Molecular Therapy
Original Article

miR-210 Enhances the Therapeutic Potential of Bone-Marrow-Derived Circulating Proangiogenic Cells in the Setting of Limb Ischemia

Marie Besnier,[1,8] Stefano Gasparino,[2,8] Rosa Vono,[2,8] Elena Sangalli,[2] Amanda Facoetti,[2] Valentina Bollati,[3] Laura Cantone,[3] Germana Zaccagnini,[4] Biagina Maimone,[4] Paola Fuschi,[4] Daniel Da Silva,[4] Michele Schiavulli,[5] Sezin Aday,[1] Massimo Caputo,[1] Paolo Madeddu,[1] Costanza Emanueli,[1,6,7] Fabio Martelli,[4,7] and Gaia Spinetti[2,7]

[1]Bristol Heart Institute, School of Clinical Science, University of Bristol, Bristol, UK; [2]Laboratory of Cardiovascular Research, IRCCS MultiMedica, Milan, Italy; [3]EPIGET Lab, Department of Clinical Sciences and Community Health, University of Milan, Milan, Italy; [4]Molecular Cardiology Laboratory, IRCCS Policlinico San Donato, San Donato, Italy; [5]AORN Santobono Pausilipon, Transfusion Medicine and Bone Marrow Transplantation Unit-Regional Reference Center for Coagulation Disorders, Napoli, Italy; [6]National Heart and Lung Institute, Imperial College London, London, UK

Therapies based on circulating proangiogenic cells (PACs) have shown promise in ischemic disease models but require further optimization to reach the bedside. Ischemia-associated hypoxia robustly increases microRNA-210 (miR-210) expression in several cell types, including endothelial cells (ECs). In ECs, miR-210 represses EphrinA3 (EFNA3), inducing proangiogenic responses. This study provides new mechanistic evidences for a role of miR-210 in PACs. PACs were obtained from either adult peripheral blood or cord blood. miR-210 expression was modulated with either an inhibitory complementary oligonucleotide (anti-miR-210) or a miRNA mimic (pre-miR-210). Scramble and absence of transfection served as controls. As expected, hypoxia increased miR-210 in PACs. *In vivo*, migration toward and adhesion to the ischemic endothelium facilitate the proangiogenic actions of transplanted PACs. *In vitro*, PAC migration toward SDF-1α/CXCL12 was impaired by anti-miR-210 and enhanced by pre-miR-210. Moreover, pre-miR-210 increased PAC adhesion to ECs and supported angiogenic responses in co-cultured ECs. These responses were not associated with changes in extracellular miR-210 and were abrogated by lentivirus-mediated EFNA3 overexpression. Finally, *ex-vivo* pre-miR-210 transfection predisposed PACs to induce post-ischemic therapeutic neovascularization and blood flow recovery in an immunodeficient mouse limb ischemia model. In conclusion, miR-210 modulates PAC functions and improves their therapeutic potential in limb ischemia.

INTRODUCTION

It has been estimated that more than 200 million people worldwide are affected by peripheral arterial disease (PAD).[1] Critical limb ischemia (CLI), the most serious form of PAD in the legs, requires foot amputation in 25% of subjects within 1 year from the diagnosis, and 25% of the patients with CLI will die during the same period.[2] Revascularization unsuitability or failure results in more severe outcomes in terms of major amputation and mortality rates, especially in subjects with diabetes mellitus.[3] Even if successful, revascularization does not prevent systemic complications (infarction or stroke).[4] Regenerative medicine could offer new solutions to this outstanding clinical need. Restoring tissue homeostasis after an ischemic event requires the control of vascular and muscular protection and regeneration, involving complex multicellular processes brought about by cells resident in muscles (vascular endothelial cells [ECs], pericytes, and satellite cells) and bone marrow (BM)-derived proangiogenic circulating cells.[5–7] These concepts are at the basis of the development of cell-based therapeutic angiogenesis for patients suffering of PAD and CLI. The outcome of a recent meta-analysis revising the efficacy of cell injection in no-option CLI patients has shown that cell therapy enhances wound healing and reduces amputation probability by 59% and 37%, respectively.[8] The therapeutic value of blood circulating BM-derived cells may be dependent on the abundance and quality of proangiogenic cells (PACs). This concept was raised by the discovery about 2 decades ago of the post-natal vasculogenic and angiogenic potential of a subpopulation of circulating mononuclear cells (MNCs) of BM origin that express CD34 and the vascular endothelial growth factor (VEGF)-A receptor kinase insert domain receptor (KDR).[9] One approach to study these PACs, also previously known as endothelial progenitor cells (EPCs), is to enrich them by culture using a medium containing EC growth factors. PACs are positive for CD45, CD34, CD31, and KDR and uptake acetylated low-density lipoproteins (LDL). When injected in immunocompromised animal models of limb or myocardial ischemia, PACs have been reported

Received 27 December 2017; accepted 5 June 2018;
https://doi.org/10.1016/j.ymthe.2018.06.003.

[7]These authors contributed equally to this work.

[8]These authors contributed equally to this work.

Correspondence: Gaia Spinetti, Laboratory of Cardiovascular Research, IRCCS MultiMedica, Via Fantoli 16/15, Milan 20138, Italy.
E-mail: gaia.spinetti@multimedica.it
Correspondence: Fabio Martelli, Molecular Cardiology Laboratory, IRCCS Policlinico San Donato, via Morandi 30, San Donato Milanese, Milan 20097, Italy.
E-mail: fabio.martelli@grupposandonato.it

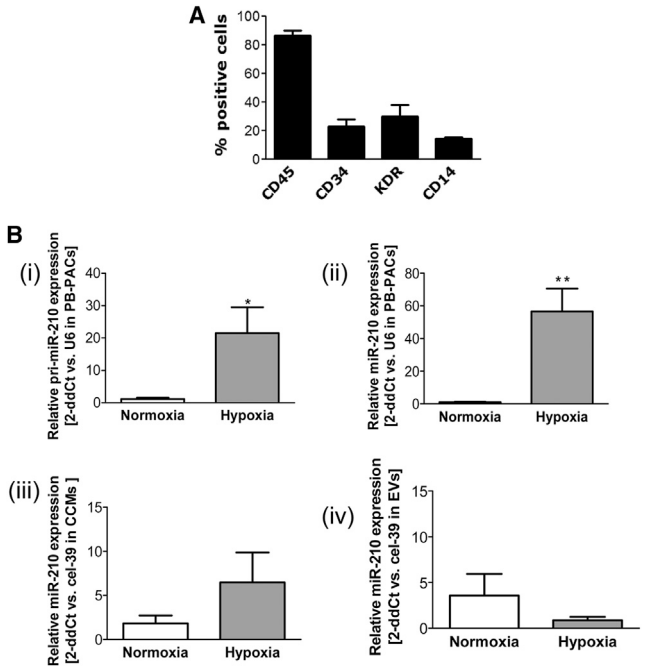

Figure 1. Hypoxia Enhances miR-210 Expression in Culture-Selected Human PACs from Peripheral Blood

(A) Cytofluorimetric characterization of peripheral blood (PB)-PACs. The bar graph shows the percentage of cells positive for hematopoietic cell marker CD45, proangiogenic cell markers CD34 and KDR, and monocyte marker CD14 (data shown as mean ± SEM, n = 4 donors). (B) Bar graph of average relative expression of (i) primary (pri)-miR-210 and (ii) mature miR-210 in PB-PACs to U6 snRNA, which was used as a normalyzer; (iii) miR-210 expression versus cel-39 spike-in gene in the unfractionated cell medium (CCM) of PB-PACs and (iv) in its extracellular vesicles (EVs); PACs were cultured 48 hr under normoxia (white bars) or hypoxia (gray bars, at 1%O_2); *$p < 0.05$ and **$p < 0.01$ versus normoxia, data shown as mean ± SEM, n = 4 donors.

to physically adhere to the endothelium and integrate in blood vessels; albeit their ability to differentiate in mature ECs is now considered limited. Additionally, PACs support angiogenesis via paracrine actions.[10] PACs represent an easily accessible, ethically justifiable, and valuable study model for autologous cell therapy strategies.[11,12] However, the translational potential of autologous adult PACs is tempered by their low abundance in the circulation, difficulties to expanding the cells *in vitro* and the negative impact of associated risk factors on the cell regenerative potential. In this context, in 2012, we proposed the possibility to improve the phenotype of adult PAC before transplantation by using microRNAs (miRs) that control intrinsic stem cell function and angiogenesis,[13] but we did not investigate miR-210.[14,15] Umbilical cord blood (UCB) represents an alternative source of PAC. Indeed, PACs are more abundant in the cord blood than in the adult blood and UCB-PACs can be more easily expanded in culture, offering obvious advantages for performing *in vivo* transplantation studies.[16,17] Additionally, UCB-PACs can be banked for future therapeutic applications benefitting the donors. UCB-PACs banking can be particularly indicated in subjects born with known congenital defects in their heart and vasculature. These patients will enter a journey of investigations and often repeated surgeries and interventions and have a higher risk of developing ischemic disease.[18]

Hypoxia, via hypoxia-inducible factor (HIF)-1α, robustly increases intracellular miR-210 expression in several tissues and cells, including ECs.[14,15] In ECs, miR-210 activates survival pathways[19–22] and enhances migratory and proangiogenic capacities.[21,23–30] We previously showed that miR-210 modulates EC by inhibiting Ephrin-A3 (EFNA3), a glycosylphosphatidyl-inositol-linked membrane-bound ligand.[21] Ephrins are a family of cell-surface ligands that interact with Eph tyrosine kinase receptors to mediate intercellular adhesion and repulsion. Ephrin-Eph interactions guide migration and positioning of the cells for proper tissue patterning during vascular development and post-natal angiogenesis. Interestingly, even if EFNA3 is inhibited by miR-210, EFNA3 was found expressed at very high levels in ischemic tissues.[31] In a cancer setting, it was recently shown that hypoxia regulates EFNA3 expression through a non-direct mechanism that involves the HIF-mediated transcriptional induction of a novel family of long-noncoding RNAs (lncRNAs) from the *EFNA3* locus.[32] In turn, lncEFNA3 would favor EFNA3 protein accumulation acting at the post-transcriptional level.[32]

This study has mechanistically investigated the expression and function of miR-210 in cultured PACs and trialled the therapeutic potential of miR-210 overexpressing PACs in an immunocompromised mouse model of LI.

RESULTS

Hypoxia Increases miR-210 in Human PACs

Adult peripheral blood (PB)-PACs were obtained from MNCs of healthy donors by culture selection in the presence of EC growth factors-rich medium. Similar to our previous studies,[13,33] cultured PB-PACs were positive for CD45, CD34, KDR, and CD14 (lipopolysaccharide [LPS] receptor, expressed prevalently on monocytic cells; Figure 1A). Following hypoxia, PB-PACs increased both the primary transcript (pri-miR-210) and mature forms of miR-210 (Figures 1Bi and 1Bii). We tested whether hypoxia increased the secretion of mature miR-210 in the conditioned medium, but no significant differences were observed in either the unfractionated medium or in the extracellular vesicles (EVs) (Figures 1Biii and 1Biv), suggesting some level of miR-210 retention in the parental cells.

Modulation of miR-210 Levels by Pre- and Anti-miR-210

To study whether miR-210 modulation had an impact on human PAC biofunctions, we transfected PB-PACs with a synthetic miR-210 sequence (pre-miR-210) or chemically modified complementary oligonucleotides (anti-miR-210) to enhance or inhibit its levels, respectively. As shown in Figure S1, both interventions efficiently modulated miR-210 levels of PB-PACs cultured.

miR-210 Does Not Modulate the Expression of HIF-1α-Regulated Genes in PACs

The hypoxia-responsive factor HIF-1α modulates miR-210 directly,[34] and it was proposed that miR-210 regulates a

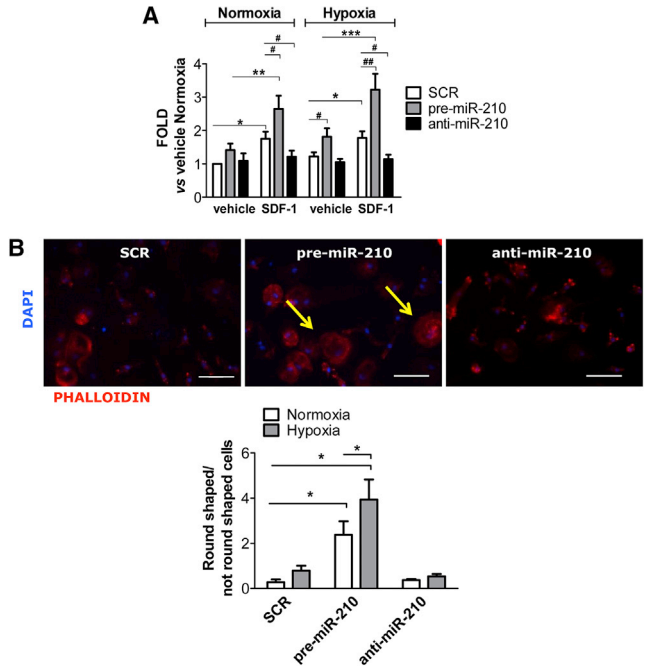

Figure 2. miR-210 Affects the Migratory Capacity and Morphology of PB-PACs

(A) Bar graph shows the capacity of PB-PACs engineered with pre- or anti-miR-210 to migrate toward SDF-1 (CXCL-12) or in the absence of chemoattratant (vehicle). *p < 0.05, **p < 0.01, ***p < 0.001 versus vehicle; #p < 0.05, ##p < 0.01 versus SCR. Data shown as mean ± SEM, n = 6 donors. (B) Alteration of cell shape in response to miR-210 modulation. Representative images of phalloidin staining: round-shaped cells are indicated by yellow arrows. Scale bars, 50 μm. Bar graph indicates the average number of round-shaped cells, *p < 0.05. Data shown as mean ± SEM, n = 5 donors.

feed-forward mechanism involving HIF-1α-regulated genes.[35–37] However, in PACs, the expression of genes under the control of HIF-1α, such as Glucose transporter 1 (*GLUT-1*), Aldolase, Fructose-Bisphosphate C (*ALDO-C*), *VEGF-A*, and Adrenomedullin (*ADM*) were not affected by forced miR-210 expression changes (Figure S2), which suggests the absence of loop in which miR-210 potentiates HIF-1α activity. The data discourages the speculation that such genes could mediate the responses induced by PAC expressing miR-210 in the adopted experimental conditions.

SDF-1α-Directed Migration of PB-PACs Is Sensitive to miR-210 Levels

After an ischemic insult, chemotactic factors are released in the circulation and PB-PACs follow the chemokine gradient to migrating toward and home at the injured tissue.[38] Stromal cell-derived factor 1 (SDF-1α) (C-X-C motif chemokine ligand [12CXCL12]) is considered to be the prototypical promigratory chemokine.[39] As shown in Figure 2A, we first validated that cultured PB-PACs migrated toward SDF-1α both in normoxic and hypoxic conditions. Moreover, pre-miR-210-transfected PB-PACs increased SDF-1α-directed cell migration both in normoxia (p = 0.0032 versus vehicle and p = 0.0058 versus SDF-1α-scramble [SCR]) and in hypoxia (p = 0.0004 versus vehicle and p = 0.0013 versus SDF-1α-SCR). Consistently, blocking miR-210 with anti-miR reduced PB-PAC migratory ability in the presence of the chemoattractant both under normoxia and hypoxia (p = 0.0105 and p = 0.0250 versus SCR, respectively). The migration toward SDF-1α requires the activation of SDF-1α cognate receptor C-X-C chemokine receptor type 4 (CXCR-4) in the parent cells.[40] Worth noting, hypoxia reportedly increases CXCR4 expression in progenitor cells.[41] Therefore, we verified if CXCR4 expression was changed in miR-210-transfected-PB-PACs. CXCR4 was effectively induced by hypoxia in PB-PACs, but not further regulated by the miR-210 changes induced by transfection with pre- or anti-miR-210 (Figures S3A and S3B).

miR-210 Modulation Affects the Interaction of PB-PACs and ECs in Co-culture

We observed morphological changes in adult PACs overexpressing miR-210, as highlighted by the staining for the cytoskeletal protein phalloidin (Figure 2B), with an increased number of flat and round-shaped cells both in normoxic or hypoxic conditions (p = 0.0176 and p = 0.0358 versus SCR, respectively). In addition, in miR-210-transfected PB-PACs hypoxia induced a further increase in the number of round-shaped cells (p = 0.0493 versus normoxia). These evidences suggest a potential effect of miR-210 on cell adhesion. Indeed, to support ECs in the angiogenic process, PB-PACs need first to adhere to the endothelium. Thus, we measured the number of PKH26 red-stained PB-PACs that were efficiently attached to a monolayer of human umbilical vein ECs (HUVECs) after 1 hr of co-culture. Hypoxia promoted PB-PAC adhesion to HUVECs (p = 0.0311 versus normoxia). Of note, miR-210 overexpression alone (p = 0.0052 versus SCR) or in combination with hypoxia (p = 0.0313 versus SCR) increased PAC adhesion. In addition, inhibiting miR-210 in PB-PACs with anti-miR prevented the enhancement of hypoxia-induced PB-PAC adhesion to ECs (Figure 3A).

Next, we investigated the possibility that PB-PACs transfected with pre-miR-210 could better support HUVEC capacity to form network structures on a Matrigel layer, a model of *in vitro* angiogenesis. When HUVECs were cultured with miR-210-overexpressing PACs, they showed a higher networking capacity both under normoxia and hypoxia (p = 0.0241 and p = 0.0003 versus SCR-PACs, respectively) (Figure 3B). Green PKH67-labeled miR-210-transfected PACs locate all around red PKH26-labeled-HUVECs, confirming their cooperation in HUVECs networking on Matrigel, suggesting that cell-cell contact is necessary for miR-210-dependent stimulation of angiogenesis by PB-PACs. Supporting this hypothesis, neither the complete cell-conditioned medium (CCM) of miR-210-transfected PB-PACs or isolated EVs obtained from miR-210-tranfected PB-PACs increased EC networking (Figures S4A and S4B). Accordingly, the number of exosome-sized EVs measured by Nanosight technology was similar in CCM from SCR, pre-miR-210, and anti-miR-210 transfected PB-PACs (Figure S4C).

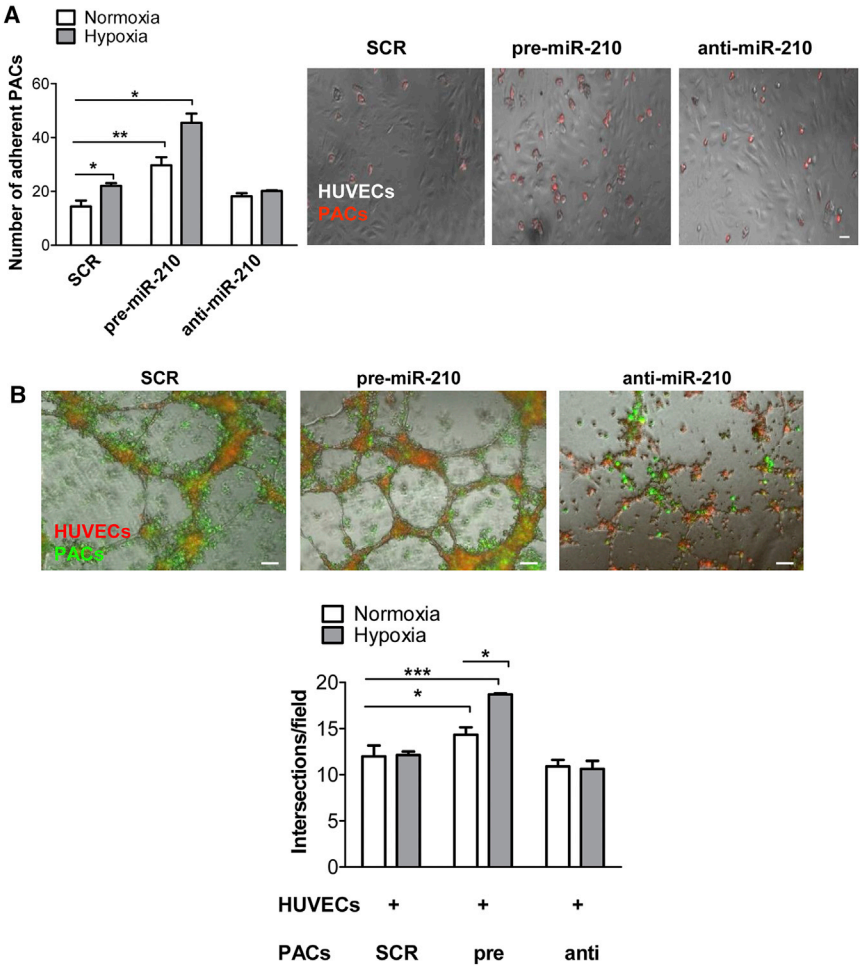

Figure 3. miR-210 Mediates PB-PACs' Interaction with Endothelial Cells

(A) miR-210-transfected PB-PAC adhesion assay to human umbilical vein endothelial cells (HUVECs). Bar graph of average cell number ± SEM (left) and representative images (right; scale bars, 100 μm). n = 3 donors. (B) Bar graph of average intersections of HUVECs cultured in the presence of engineered PB-PACs (bottom) and representative images (upper; scale bars, 100 μm). Red, PKH26 dye (HUVECs); green, PKH67 dye (PACs). *$p < 0.05$; ***$p < 0.001$, data shown as mean ± SEM, n = 4 donors.

EFNA3 Overexpression Prevents miR-210-Induced Migration and Adhesion of PACs *In Vitro*

EFNA3 is directly targeted by miR-210 for repression.[21,42,43] In ECs, miR-210 does not reduce mRNA level but decreases EFNA3 protein.[21] In line with that, both EFNA3 mRNA and miR-210 were found upregulated in the ischemic brain.[31] Interestingly, in hypoxic metastatic tumors, EFNA3 protein expression was reported to be additionally regulated by HIF-induced expression of lncRNAs transcribed from the *EFNA3* locus.[32] Here, we investigated whether a similar mechanism occurred in PACs. Using qPCR primers able to discriminate the mRNA and lncRNA transcripts (Figure S5A), we observed that in comparison to EFNA mRNA, lncEFNA3 expression was negligible in PACs (data not shown). Moreover, in PACs, neither hypoxia nor forced miR-210 expressional changes affected the expression of EFNA3 mRNA or of lncEFNA3 (Figures 4Ai and 4Aii). However, EFNA3 protein levels, measured by immunofluorescence staining, were responsive to miR-210 expression (Figure 4B). To study whether EFNA3 repression in PB-PACs is important for miR-210-induced migration and adhesion, we attempted to rescue EFNA3 expression using a lentiviral vector (LV). The successful increase in EFNA3 mRNA after LV-mediated gene transfer of PACs was confirmed by qPCR (Figures 5A and 5B).

Figure 5C shows that the concomitant upregulation of the duo EFNA3/miR-210 prevented the promigratory function of miR-210, especially in the presence of the chemoattractant SDF-1α. A similar effect was also observed in the cell-adhesion protocol (Figure 5D), where pre-miR-210 transfection increases PB-PACs adhesion. Interestingly, EFNA3 overexpression prevented miR-210-induced adhesion to HUVECs (Figure 5D). EFNA3 action can be mediated by the engagement of its EPHA4 receptor.[44] Therefore, we additionally analyzed the expression of EPHA4 in PACs. We could not detect any significant EPHA4 expressional change associated with PAC transfection of SCR, pre-miR-210 or anti-miR-210 under normoxia and hypoxia (Figure S5B). Collectively, the above data indicate that miR-210 upregulation targets EFNA3, and this decrease is necessary for miR-210 promigratory and proadhesive functions.

miR-210 Enhances the Therapeutic Potential of PACs in a Mouse Model of LI

For the *in vivo* protocol, we employed UCB-PACs. The UCB-PACs were first characterized for the expression of the classical markers already reported in PB-PACs (see Figure 1A). Consistent with the literature, a high proportion of UCB-derived cells (40%) were CD34 positive and (40%) of the cells were KDR positive, a lower proportion of the cells were CD45, while only few cells expressed CD14 (Figure S6A).[17,45] Next, we sought confirmation that the new model of UCB-PACs behaved similarly to PB-PACs characterized in this study. In detail, UCB-PACs responded to hypoxia with increased levels of miR-210 (Figure S6B). Furthermore, UCB-PACs could be efficiently transfected with pre-miR-210 or anti-miR-210, overexpressing or inhibiting miR-210, respectively (Figure S6C). Functionally, we also verified that in UCB-PACs pre-miR-210 transfection increased the capacity to support HUVEC networking on Matrigel, while anti-miR-210 elicited the opposite effect (Figure S6D).

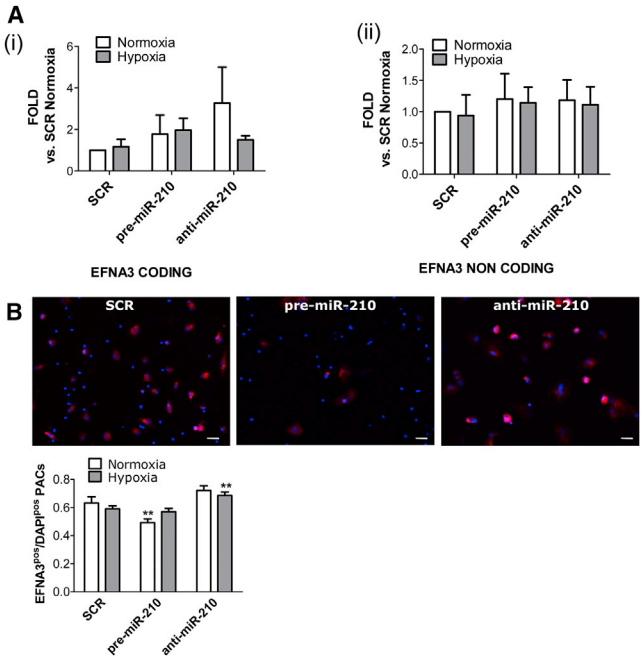

Figure 4. Analysis of Coding and Non-coding EFNA3 Isoforms following miR-210 Modulation

(A) The expression of both coding and non-coding EFNA3 has been analyzed following miR-210 modulation in PB-PACs under normoxia and hypoxia. Real-time qPCR showed no mRNA modulation for coding (i) and non-coding EFNA3 over UCB housekeeping gene. Data shown as mean ± SEM, n = 4 donors. (B) Coding EFNA3 quantification by immunofluorescence staining confirmed EFNA3 is controlled by miR-210 modulation under normoxia but not hypoxia. **p < 0.01 versus SCR normoxia and pre-miR-210 normoxia; data shown as mean ± SEM, n = 4 donors.

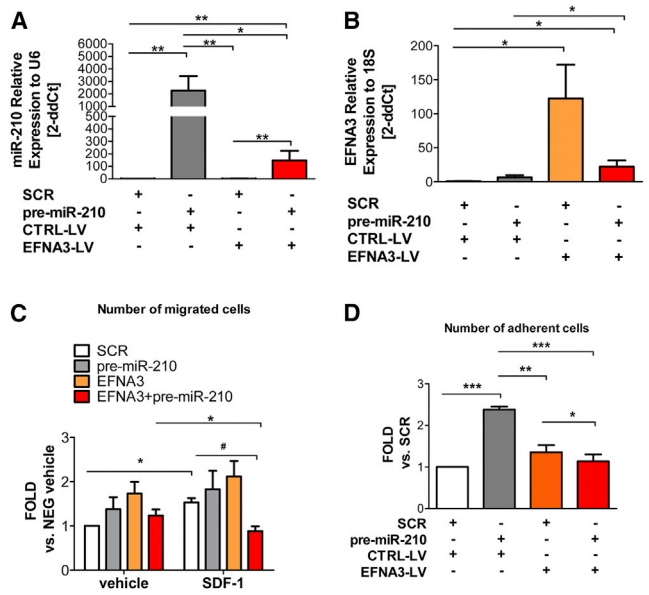

Figure 5. mir-210 Overexpression Mediates PB-PACs Migratory and Adhesive Functions, Which Are Impaired by Concomitant EFNA3 Overexpression

(A) Analysis of miR-210 expression in PACs infected for 24 hr with EFNA3-bearing lentivirus (LV) and transfected with pre-miR-210. Bars represent treatment respectively with empty vector lentivirus (white bar), empty vector lentivirus + pre-miR-210 (gray bar), EFNA3 lentivirus (orange bar), and EFNA3 lentivirus + pre-miR-210 (red bar). Data expressed as mean 2ddCts ± SEM versus U6 snRNA. Concentration of viral particles 1 MOI. n = 5 donors. *p < 0.05, **p < 0.01. (B) Analysis of EFNA3 mRNA by qPCR in PACs treated as described in (A). Data expressed as mean 2ddCts ± SEM versus U6 snRNA. n = 4 donors. *p < 0.05. Lentivirus-mediated EFNA3 overexpression in PB-PACs abrogated the positive impacts induced by miR-210 overexpression on migration (C) and adhesion (D). For (C), *p < 0.05 versus vehicle, #p < 0.05 versus SCR. n = 4 donors. For (D) *p < 0.05, **p < 0.01, ***p < 0.001; data shown as mean ± SEM, n = 5 donors.

Next, the therapeutic potential of UCB-PACs expressing different miR-210 levels was assessed *in vivo*. Transplantation of UCB-PACs overexpressing miR-210 into ischemic muscles improved post-ischemic blood flow recovery (Figure 6A) and increased microvascular density in ischemic muscles (Figure 6B). In this experimental setting, we did not observe therapeutic responses associated with injection of PACs transfected with either scrambled or anti-miR-210 oligonucleotides (Figure 6B). Comparisons between responses induced by naive UCB-PACs and EC basal medium-2 (EBM-2) control medium showed no difference, suggesting that the lack of therapeutic effect of PACs transplantation alone was not due to a negative effect of the transfection on the cell function (Figures S7A and S7B). Even if we cannot provide data on circulating miR-210 in immunocompromised mice receiving PAC transplantation, we measured miR-210 by qPCR in the plasma of in C57BL/6 mice subjected for 3 days to experimental ischemia (Figure S7C). Data confirm an increase of miR-210 also in the plasma of ischemic mice.

DISCUSSION

In this investigation, we demonstrated the potential of miR-210 to improve migratory and adhesive abilities of PACs, with positive consequences on angiogenesis *in vitro* and *in vivo*.

miR-210 is historically regarded as the master hypoxamiR. Indeed, endogenous miR-210 has been proven to be dramatically increased by hypoxia in virtually any tested cell type.[14,15] Adult and cord blood PACs are not exception, as demonstrated here for the first time. Since high miR-210 levels in ECs were associated with activation of angiogenesis, we investigated whether bearing high miR-210 was stimulating PAC functions, with the final goal of improving cell-based regenerative therapy approaches.[46] Specifically, *in vitro*, we worked with PACs derived from two sources: adult PB and UCB. By contrast, for *in vivo* experiments, we focused on UCB-PACs, capitalizing from the University of Bristol research program employing perinatal material for stem cells and tissue engineering therapies dedicated to patients born with congenital heart defects, although the cells used here were all from healthy donors. We previously characterized human adult PACs in several studies and demonstrated that these cells express a series of miRs that regulate angiogenesis. We already proved that PACs can be engineered with either anti-miRs (to miR-15a and 16) or tissue kallikrein to improve their migratory capacity and *in vivo* proangiogenic potential.[13,33] Here, we provide novel evidence that

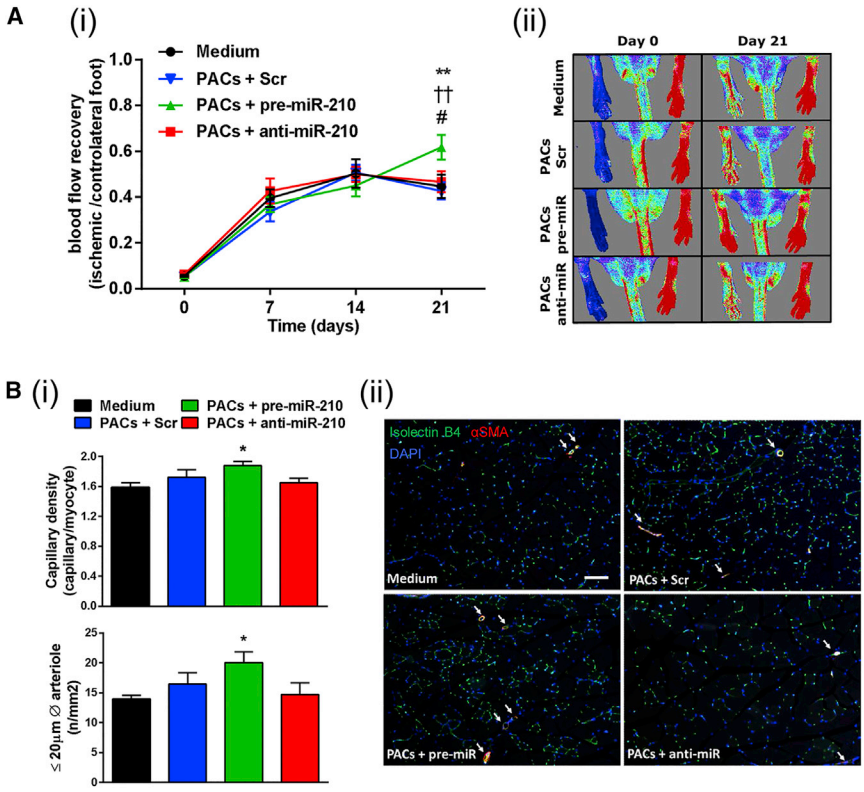

Figure 6. UCB-PACs Engineered *Ex Vivo* to Overexpress miR-210 Show a Higher Therapeutic Potential for Vascular Repair in an Immunocompromised Mouse Model of Unilateral Limb Ischemia

UCB-PACs were engineered *ex vivo* with scramble control (SCR) and pre- or anti-miR-210. Engineered UCB-PACs or fresh cell medium were injected in the ischemic adductor muscle of mice with surgically induced unilateral limb ischemia. (A) Post-ischemic blood flow recovery: (i) Time course of blood flow recovery (calculated as the ratio of blood flow in ischemic to contralateral foot) (data shown as mean ± SEM, n = 12–14/group), (ii) representative color laser Doppler flowmetry images at 0 and 21 days from surgery. (B) Analyses of capillary and arteriole density in ischemic muscles: (i) bar graphs showing capillary and arteriole (≤20 µm diameter) density in ischemic adductor muscles at 21 days post-ischemia (data shown as mean ± SEM, n = 8–10/group). (ii) Representative ischemic muscle sections stained with the endothelial marker isolectin B4 (green fluorescent) and an antibody for α-smooth muscle actin (red fluorescent) to identify smooth muscle cells in the arterial wall (scale bar, 100 µm). Arterioles are shown by white arrows. Data are expressed as mean ± SEM. *$p < 0.05$, **$p < 0.01$, PACs + pre-miR-210 versus medium; ††$p < 0.01$, PACs + pre-miR-210 versus PACs + SCR; #$p < 0.05$, PACs + pre-miR-210 versus PACs + anti-miR-210.

miR-210 overexpression enhanced PAC migration *in vitro*. This is associated with a remodeling of the cell shape and reduced EFNA3 protein expression. EFNA3 is a well-characterized miR-210 target.[21,31,42,43] Gómez-Maldonado et al.[32] recently proposed that lncEFNA3 isoforms are induced by hypoxia and positively regulate EFNA3 expression. However, in PACs, lncEFNA3 expression was much lower than the EFNA3 mRNA, and lncEFNA3 expression was not modulated by hypoxia or miR-210.

Overriding the miR-210-induced EFNA3 down-modulation was shown to prevent EC chemotaxis and/or angiogenesis.[21,42] We confirmed this in PACs by simultaneously overexpressing miR-210 and EFNA3. In details, we showed that LV-induced increase in EFNA3 were sufficient to contrast the promigratory and proadhesive effects induced by pre-miR-210 transfection in PACs. The data provide evidence of the importance of EFNA3-miR-210 interaction in regulating the behavior of miR-210-engineered PACs. However, further experiments are needed to clarify the EFNA3-miR-210 relationship under physiological conditions.

The possibility to use miR engineering to manipulate stem cells into more powerful therapeutic tools is attractive. We had already validated the feasibility and potential of manipulating miR-17 expression in UCB-PACs.[47] Moreover, miR-210 overexpression already proved utilitarian in mesenchymal stromal cells (MSCs).[22,48] miR-210 modulation was associated with increased cell survival, in keeping with the inhibition of the miR-210 target, caspase-8-associated protein-2.[35] In PACs, miR-210 expressional changes did not impact cell proliferation and survival (data not shown), suggesting that miR-210 function is highly context dependent.[14,49]

PACs have been shown to activate resident ECs, at least in part through vesicle-mediated transfer of miRs.[50–52] Moreover, increased miR-210 microvesicle-associated levels have been observed in a variety of cell types exposed to hypoxia.[42,53–56] However, at a difference with recent EV literature,[42,57–59] the EV cargo of PACs did not appear to reflect miR-210 changes in the parent cells. Moreover, our data provide evidence against the hypothesis that PAC-released extracellular miR-210 of either endogenous or exogenous origin mediates the angiogenic responses to PACs. This represents a relevant control, because it allows us to exclude that miR-210 released by overloaded PACs after pre-miR-210 transfection could account for the response observed in ECs co-cultured with PACs.

miR-210 overexpression in PB-PACs stimulated changes in their cytoskeleton and promoted angiogenesis response by co-cultured EC. However, anti-miR-210 treatment of PACs did not impact on this effect. While we do not have an exhaustive explanation of the underlying mechanisms, we speculate that the level of miR-210 necessary to promote such PAC actions is maintained after anti-miR-210. Another possible interpretation is that miR-210 might be sufficient, but not necessary, for certain PB-PAC functions. It is also worth

noting that the response to anti-miR-210 might be cell type dependent. In fact, miR-210 inhibition decreased the ability of UCB-PACs to stimulate the capillary-like tube formation in co-cultured ECs.

To validate *in vivo* the proangiogenic function played by miR-210 in PACs, we employed UCB-PACs, which are currently considered a particularly attractive cell system for clinical application.[16,17] Additionally, it was reported that, in comparison with adult PACs, human UCB-PACs induce growth of more durable blood vessels in mouse (up to 4 months versus 3 weeks for adult cell PACs).[60] Moreover, data obtained studying UCB-PACs might be more easily transferred to a future clinical setting, since the UCB is currently an approved source of cell for regenerative therapy and it is banked in several countries.[18] *In vitro* experiments confirmed that in UCB-PACs miR-210 was readily induced by hypoxia and that its expression stimulated the network formation by co-cultured ECs. Since we found that the miR-210-PACs supports angiogenesis by cell-to-cell contact *in vitro*, we injected the cells directly into the ischemic tissue, to allow cell contact to happen in the ischemic limb vasculature. We acknowledge that this site of injection creates an unfavorable environment for cell survival, as previously described.[61] Pre-miR-210-overexpressing UCB-PACs increased post-ischemic reparative angiogenesis and blood flow recovery. Interestingly, the effect seems to be stronger on small arteriole development as compare to capillary density. We believe this reveals an interesting effect of miR-210-engineered PACs for which we do not have a clear mechanism, and that would be interesting to explore further.

We could not measure a change of miR-210 expression *in vitro* in the conditioned medium or in the extracellular vesicles of miR-210-PACs. Nonetheless, we cannot exclude that after transplantation, PAC start to release miR-210, contributing to the effect on vascular repair. In line with this possibility, we found that endogenous cells, of not-yet-defined types, appear to contribute to LI-induced increases in circulating miR-210 levels observed in mouse PB-derived plasma. Naive PB-PACs and CB-PACs have shown beneficial effects in pre-clinical and clinical studies.[62] We have been previously unable to replicate such responses with adult PB-PACs.[13] Similarly, we here report absence of *in vivo* therapeutic responses to untreated UCB-PACs. This could be explained taking into account that different studies might differ for methods of cells isolation, surgical techniques to induce LI, animal background and sex, and site of cell injection. Moreover, the number of cells injected in mice usually varies between 2×10^5 to 1×10^6 cells.[47,63,64] We injected 2×10^5 cells, which is at the lower boundary of the aforementioned range.

All together, our data point to miR-210 as way to improve PAC functional activities. We therefore propose that miR-210-engineering of PACs should be further explored as a way to improve cellular regenerative therapies in ischemic diseases. miR-210 overexpression in PACs and other regenerative cells could also aid in tissue engineering. Example scenarios of the latter would be using miR-210-expressing PACs to support vascularization of scaffolds, as well as of vascular and heart valve conducts, thus responding to the demands regenerative medicine must meet to correct acquired defects (like CLI and ischemic heart disease), while expanding to address the needs presented by surgery for congenital heart and vessel defects.

MATERIALS AND METHODS

Cell Isolation, Culture, and Treatments

Human blood circulating PACs were isolated and cultured as previously described[13,33] from a small cohort of healthy subjects. The study protocol complied with principles of the Declaration of Helsinki and was covered by institutional ethical approval (11/2015 Cardiovascolare). For this study, 25 patients were enrolled with a mean age (SEM) of 41.5 (2.5) years. 40% of the patients were male and 60% were female. The collection of human UCB used in this study was approved by the North Somerset and South Bristol Research Ethics Committee (Research Ethic Committee [REC] reference 11/H0107/4). A total of 11 donors were recruited at a gestational age comprised between 39 and 40 weeks. The cells were isolated following the same protocol than used for the isolation of PACs from adult peripheral blood. In brief, human UCB MNCs were isolated by gradient centrifugation on Histopaque-1077 density medium (Sigma). For enrichment of the PACs, 1×10^7 MNCs/well were plated on fibronectin (Sigma)-coated 6-well plates (BD Falcon) and cultured for 4 days in EBM-2, supplemented with EC growth medium-2 micro vascular (EGM-2MV) SingleQuots, 10% fetal bovine serum (FBS) (EGM-2MV; Cambrex), and 1% penicillin and streptomycin. At that time, non-adherent cells were removed by two washes of PBS. Cells were then cultured for 6–8 days before being transfected with a non-targeting sequence, also identified as SCR throughout the manuscript (AM4611, Silencer Negative Control, Ambion), pre-miR-210-3p (PM10516, Ambion), or anti-miR-210-3p (AM10516, Ambion), 50 nmol/L using Gensilencer Transfection reagent (Genlantis) using the manufacturer's protocol. Three days after transfection, cells were exposed to hypoxia (5% CO_2, 1% O_2) for 3 days before being harvested for further analysis. In parallel experiments, we assessed the efficiency of PAC transfection by transfecting fluorescently labeled miR-mimic (miR-mimic-Pe-Cy3) (Applied Biosystems). The percentage of transfected PACs was greater than 95%.

HUVECs were purchased by Invitrogen and cultured in EBM-2 medium, supplemented with EGM-2 SingleQuots (Lonza) and 2% FBS (Gibco).

RNA Extraction and Expressional Analyses

RNA was extracted from cultured cells using miRNeasy Mini Kit (QIAGEN) following the manufacturer's instructions. The concentration of total RNA was determined using the Nanodrop ND1000 Spectrophotometer (Thermo Scientific). RNA reverse transcription to measure miRs was performed with the TaqManmiR reverse transcription kit following the manufacturer's instructions (Applied Biosystems). miR-210 (hsa-mir-210; assay ID: 000512) expression was analyzed by the QuantStudio 6 Flex Real-Time PCR System (Applied Biosystems) and normalized to the U6 small nucleolar RNA (U6 small nucleolar RNA [snRNA]; assay ID: 001973).

For gene expression analyses, single-strand cDNA was synthesized from 1 μg of total RNA using TaqMan Reverse Transcription reagents (Applied Biosystems). qRT-PCR was performed with the QuantStudio 6 Flex Real-Time PCR System (Applied Biosystems) using the following primers: 18 s rRNA (forward, 5′-CGCAGCT AGGAATAATGGAATAGG-3′; reverse, 5′-CATGGCCTCAGTTCC GAAA-3′); CXCR4 (forward, 5′-CAGTGGCCGACCTCCTCTT-3′; reverse, 5′-GGACTGCCTTGCATAGGAAGTT-3′); EFNA3 (forward, 5′-CTCTCCCCCAGTTCACCAT-3′; reverse, 5′-TGAGGGTT CTCTCCCTCAAA-3′); VEGF-A (forward, 5′-CAACATCACCAT GCAGATTATGC-3′; reverse, 5′-TCGGCTTGGCACATTTTTC TTGT-3′); ALDO (forward, 5′-GGCTGCCACTGAGGAGTTC-3′; reverse, 5′-CTGCTGCTCCACCATCTTCT-3′); GLUT-1 (forward, 5′-GATTGGCTCCTTCTCTGTGG-3′; reverse, 5′-TCAAAGGACTT GCCCAGTTT-3′); ADM (forward, 5′-GGAAGAGGGAACTGCG GATGT-3′; reverse, 5′-GGCATCCGGATTCACCCTCCTAGC-3′). Data were normalized to 18S ribosomal RNA as an endogenous control. For miR-210 and gene expression, each PCR reaction was performed in duplicate and analyzed by the 2ddCt method.[65,66] For the investigation of coding and non-coding EFNA3 isoforms and EPHA4, the following primers pairs were designed: coding EFNA3 (forward, 5′-CACTCTCCCCCAGTTCACCAT -3′; reverse, 5′-CGCTGATGCTCTTCTCAAGCT-3′); non-coding EFNA3 (forward, 5′-AGTTTGGGCTGCGGAGAATC-3′; reverse, 5′-GCAGAC GAACACCTTCATCCT-3′); EPHA4 (forward, 5′-AGCAGCCAC TCAGGCAAC-3′; reverse, 5′-ACGAAAATAGGGCGAAATAG AA-3′). Expression was normalized to ubiquitin C (UCB) housekeeping gene.

FACS Analyses

For CXCR4 analysis, PACs (2×10^5 cells) were stained with 5 μL of CXCR4 (allophycocyanin [APC]) antibody (BD Biosciences). After 15 min incubation at room temperature in the dark, cells were washed, resuspended in PBS, and analyzed. Cells were analyzed using a FACSCanto flow cytometer with the FACSDiva software (both from BD Biosciences).

For the characterization of peripheral and cord blood PACs, 10^4 cells were incubated with human receptor FC block (eBioscience; 14-9161-71) for 5 min at room temperature. Cells were stained using 1:20 dilution of CD45-APC-Cy7 (BD Biosciences, #560178, 1:20), CD34-PE-Cy7 (BD Biosciences, #348811), KDR-PE (R&D System, FAB357P), and CD45/CD14-FITC/PE (BD Biosciences, BD Simultest 342408) in staining buffer (PBS supplemented with 0.5% bovine serum albumin) for 15 min at room temperature. Cells were washed twice and resuspended in staining buffer before being analyzed on AceaNovocyte flow cytometer. Fluorescence minus one control were used to determine positive staining. The quantification of the antigenic profile was performed using the FlowJo v10 software (FlowJo).

Migration Assay

For PACs migration assay, 5 μm pore-size filter-equipped transwell chambers (Corning) coated with fibronectin 2 μg/mL were used. Cells (7.5×10^4) were placed in the upper chamber and allowed to migrate toward SDF-1α (R&D) (100 ng/mL) or vehicle (control) for 16 hr at 37°C. The cells on the upper part of the filter were scraped away before fixing the filter. The lower side of the filter (containing the migrated cells) was mounted with Vectashield containing DAPI. For each chamber, migrated cells were counted in 5 random fields at 20× magnification. Migration data are expressed as the number of cells migrated per field toward the specific chemoattractant versus the number of cells migrated both in absence of stimulus and normoxia. Each experiment was performed in duplicate. Fluorescence was visualized and captured using AXIO OBSERVER A1 microscope equipped with digital image processing software (AxioVision Imaging System), both from Zeiss.

Adhesion Assay

HUVECs (2.5×10^4) were seeded and cultured for 24 hr in 96-well tissue culture plates (BD Falcon) in complete EGM-2 (Lonza) with 2% FBS (Gibco). PACs (2.5×10^4) were PKH26 red-stained (Sigma, stained according to the manufacturer's instructions) and added to the HUVECs layer. After 1 hr of co-culture at 37°C, cells were washed gently with PBS, and cell adhesion was quantified by counting adherent red fluorescent-PACs (magnification 10×). Each experiment was performed in duplicate. Fluorescence was visualized and captured using AXIO OBSERVER A1 microscope equipped with digital image-processing software (AxioVision Imaging System), both from Zeiss.

In Vitro Angiogenesis

Capillary-like network formation assay: 5×10^4 PACs were added to 8-well chamber slides (Nunc) precoated with 150 μL Matrigel (Becton Dickinson), together with 5×10^4 HUVECs in a total volume of 150 μL EBM-2 (Lonza) with 0.1% bovine serum albumin (BSA) (Sigma). After 5 hr incubation at 37°C, PACs' effect on network formation from HUVECs was measured by counting the number of intersection points in 10 microphotographs of random view fields (magnification 20×). Similar assays were performed adding 50 μL CCM or 50 μL of PBS containing purified extracellular microvesicles obtained from PACs to the HUVECs in 50 μL EBM-2 0.1% BSA. For double-stained pictures, 5×10^4 HUVECs and 5×10^4 PACs were stained with PKH26 red and PKH67 green, respectively, according to the manufacturer's advices prior to co-culture on matrigel. The assays were performed in duplicate wells. Microphotographs were visualized and captured using AXIO OBSERVER A1 microscope equipped with digital image processing software (AxioVision Imaging System), both from Zeiss.

Extracellular Microvesicle Isolation and Quantification

Cell conditioned medium (CCM) was processed for EV collection and ultrapurification, as described.[67] For CCM, cells were removed by centrifugation ($500 \times g$, 5 min), then CCM was clarified by centrifugation ($2{,}000 \times g$, 30 min, followed by $12{,}000 \times g$, 45 min, at 4°C). EVs were collected by ultracentrifugation ($110{,}000 \times g$, 3 hr), washed in PBS, and pelleted. The purified EV fraction was re-suspended in

100 μL PBS for use. EV purity and amount (normalized on the number of cultured cells) were confirmed by NanoSight technology.[68]

Immunofluorescence Analysis

PACs were washed with PBS and fixed with 4% paraformaldehyde (Electron Microscopy Sciences). Cells were then incubated with 10% goat serum (Sigma) at 25°C for 30 min, washed with PBS, and incubated with a rabbit anti-EFNA3 antibody (1:300) in PBS overnight at 4°C. PACs were then washed with PBS and incubated with goat anti-rabbit immunoglobulin G (IgG) (H+L) secondary antibody, Alexa Fluor 555 conjugate (Thermo Fisher Scientific) (1:200) in PBS for 1 hr at 37°C. For phalloidin staining, cells were permeabilized with 0.1% Triton X-100 following fixing, then washed, blocked with 10% goat serum as described above, and incubated 40 min with tetramethylrhodamine B isothiocyanate-conjugated phalloidin, which directly binds cytoskekletal F-actin. Fluorescence was visualized and captured using an AXIO OBSERVER A1 microscope equipped with digital image processing software (AxioVision Imaging System), both from Zeiss.

Lentiviral Packaging, Preparation, and Transduction of PACs

Human embryonic kidney cells (HEK293T) were purchased by Sigma and cultured accordingly to Sigma protocols in DMEM 4.5 g/L glucose and 10% FBS (Gibco) with sodium pyruvate 100 mM (100×), non-essential aminoacid solution (NEAA, 100×), and penicillin streptomycin (100×) (all from Sigma). The day before, 2.5×10^6 HEK293T were plated in 100-mm dishes (BD Falcon); when cells reached 70%–80% confluence, fresh medium was replaced. For transfection, two tubes were prepared each with $CaCl_2$ 2.5 M, *REV* containing plasmid (pREV, 0.64 μg), *MDL* containing plasmid (pMDL, 0.64 μg), *VSVG* containing plasmid (pVSVG, 0.64 μg), and *EFNA3* containing plasmid (pEFNA3, 3.2 μg) or CTRL empty plasmid (pCTRL, 3.2 μg). Each tube was then mixed with Hank's buffer solution (HBS) 2× and incubated for 15 min at 25°C. Each mixture was used for transfection of HEK293T. Lentivirus titration was performed by transducing HEK293T cells with concentrated particles in the presence of 4 cμg/mL polybrene and measuring GFP expression after 3 days by flow cytometry. Cells were then incubated overnight at 37°C, then the medium was replaced, and 24 hr later cell supernatants containing the virus were harvested and filtered using a 0.45-μm sterile filters (Millipore).

PACs were transduced with lentivirus at 1 MOI concentration 24 hr after the end of the transfection with miR-210. The day of transduction PACs were washed with PBS and EFNA3 (or CTRL) lentivirus plus polybrene (final concentration 8 μg/mL) (Sigma) were added. 4 hr after infection, an equal volume of complete PACs medium was added. Cells were selected with puromycine (1 μg/mL) (Calbiochem) after 48 hr from transduction.

Surgical Model of LI in Mice

The experiments involving mice were performed in accordance with the Animal (Scientific Procedures) Act (UK) of 1986 prepared by the Institute of Laboratory Animal Resources and covered under the UK Home Office Project license PPL/30/2811 and personal licenses. Experiments were performed by a blind investigator. Three-month-old immunocompromised CD1-Foxn1nu male mice (Charles River, UK; n = 12–14 mice/group) or C57BL6 mice (Charles River, Italy, n = 3–5/group) underwent surgical induction of unilateral LI by performing dissection of the left femoral artery, as we reported previously.[69] Immediately after LI induction, CD1-Foxn1nu mice received 2×10^5 PACs from cord blood from three different donors, injected into the adductor muscle. The superficial blood flow to both ischemic and non-ischemic feet was measured using a high-resolution laser color Doppler imaging system (Moor LDI2, Moor Instruments) in anesthetized animals with 1% isoflurane at days 0, 7, 14, and 21 after induction of LI. The ratio of blood flow between the ischemic and contralateral foot was calculated to use as an index of percentage blood flow recovery. At day 21, mice under terminal anesthesia were perfusion-fixed successively with 6 mL of 0.05 M EDTA and 10 mL of 10% formalin solution. Limb muscles were harvested and stored in PFA 4% overnight at room temperature then washed with PBS and finally treated with 30% sucrose overnight at 4°C. The tissue samples were then embedded in optical cutting temperature (OCT) compound and stored at −80°C until histological and immunohistochemical analyses. C57BL6 mice were used for plasma miR experiments, as previously reported.[70]

Immunohistology Analysis on Ischemic Limb Muscles

The functional impact of engineered PACs on treatment of CD1-Foxn1nu ischemic mice was assessed by measuring capillary and arteriole density in the adductor muscle. Eight-micrometer-thick muscle sections were stained using biotin-conjugated Isolectin B4 (from GriffoniaSimplicifolia; Thermo Fisher Scientific) and streptavidin-conjugated Alexa 488 (Thermo Fisher Scientific) antibodies to detect capillaries. Arterioles were identified by staining of α-smooth muscle actin (α-SMA-Cye3; Sigma) and wheat germ agglutinin-Alexa 647 (Thermo Fischer Scientific) was used to count the muscle fibers. Nuclei were stained with DAPI. The slides were mounted using Fluoromount-G (eBioscience). The relative number of positive cells was counted in ten randomly selected high-power fields (magnification 200×) using a Zeiss inverted fluorescence microscope. Analyses were performed using muscles from eight mice per group. Capillary density was expressed in as capillary-number-to-myofiber-number ratio. Arteriole density was expressed as number per mm square. Quantification was conducted by investigator blinded.

Statistical Analyses

Data are presented as mean ± SEM, and n refers to the number of donors of cells for *in vitro* experiments and number of animals for the *in vivo* analyses that are indicated in the figure legends. Statistical analyses and graphical representations were performed with appropriate software (GraphPad Prism). For molecular characterization and functional assessment of PACs, paired t test was used. Significance level was set at $p < 0.05$. For statistical comparison in animal studies, correlated outcome analysis was used to measure differences in between groups in blood flow recovery in the *in vivo* model of

mouse CLI. For histology analysis of capillary and arteriole density, one-way ANOVA with post-hoc Dunnett's test was used.

SUPPLEMENTAL INFORMATION

Supplemental Information includes seven figures and can be found with this article online at https://doi.org/10.1016/j.ymthe.2018.06.003.

AUTHOR CONTRIBUTIONS

Conceptualization, F.M., G.S., C.E.; Methodology, G.S., F.M., C.E., S.G., E.S.; Investigation, S.G., E.S., R.V., L.C., M.B., M.C., V.B., B.M., G.Z., S.A., P.F., A.F., M.S., D.D.S.; Writing – Original Draft, S.G., M.B., R.V., G.S.; Writing – Review and Editing, G.S., C.E., F.M.; P.M.; Supervision, F.M., C.E., P.M., G.S.; Funding Acquisition, F.M., C.E., P.M.

ACKNOWLEDGMENTS

We are grateful to Huidong Jia and Dominga Iacobazzi (University of Bristol) for support in cord blood collection. We acknowledge the assistance of Dr. Andrew Herman and Lorena Sueiro Ballesteros (University of Bristol Flow Cytometry Facility) for their contribution to the characterization of human cord-blood-derived cells. This work was funded by the Italian Ministry of Health Ricerca Corrente to the IRCCS MultiMedica and IRCCS Policlinico San Donato and the following grants: RF-2011-02347907 and PE-2011-02348537 (all to F.M.), Telethon-Italy (GGP14092 to F.M.), AFM-Telethon (18477 to F.M.), the Cariplo Foundation (2016-0922 to P.M.), the British Heart Foundation (BHF) Centre of Vascular Regeneration (CVR; to C.E. and P.M.), the Leducq Foundation Transatlantic Network of Excellence in Vascular microRNAs (MIRVAD-CE), BHF Chair and programme grant awards (CH/15/1/31199 and RG/15/5/31446 to C.E. and CH/1/32804 to M.C.), and the National Institute for Health Research (NIHR) Bristol Biomedical Research Centre (BRC) Cardiovascular Unit (to M.C., P.M., and C.E.). This study was supported by the NIHR Biomedical Research Centre at University Hospitals Bristol NHS Foundation Trust and the University of Bristol. The views expressed in this publication are those of the author(s) and not necessarily those of the NHS, the National Institute for Health Research, or the Department of Health and Social Care.

REFERENCES

1. Rooke, T.W., Hirsch, A.T., Misra, S., Sidawy, A.N., Beckman, J.A., Findeiss, L., Golzarian, J., Gornik, H.L., Jaff, M.R., Moneta, G.L., et al.; American College of Cardiology Foundation Task Force; American Heart Association Task Force (2013). Management of patients with peripheral artery disease (compilation of 2005 and 2011 ACCF/AHA Guideline Recommendations): a report of the American College of Cardiology Foundation/American Heart Association Task Force on Practice Guidelines. J. Am. Coll. Cardiol. *61*, 1555–1570.

2. Hirsch, A.T., Haskal, Z.J., Hertzer, N.R., Bakal, C.W., Creager, M.A., Halperin, J.L., Hiratzka, L.F., Murphy, W.R., Olin, J.W., Puschett, J.B., et al.; American Association for Vascular Surgery; Society for Vascular Surgery; Society for Cardiovascular Angiography and Interventions; Society for Vascular Medicine and Biology; Society of Interventional Radiology; ACC/AHA Task Force on Practice Guidelines Writing Committee to Develop Guidelines for the Management of Patients With Peripheral Arterial Disease; American Association of Cardiovascular and Pulmonary Rehabilitation; National Heart, Lung, and Blood Institute; Society for Vascular Nursing; TransAtlantic Inter-Society Consensus; Vascular Disease Foundation (2006). ACC/AHA 2005 Practice Guidelines for the management of patients with peripheral arterial disease (lower extremity, renal, mesenteric, and abdominal aortic): a collaborative report from the American Association for Vascular Surgery/Society for Vascular Surgery, Society for Cardiovascular Angiography and Interventions, Society for Vascular Medicine and Biology, Society of Interventional Radiology, and the ACC/AHA Task Force on Practice Guidelines (Writing Committee to Develop Guidelines for the Management of Patients With Peripheral Arterial Disease): endorsed by the American Association of Cardiovascular and Pulmonary Rehabilitation; National Heart, Lung, and Blood Institute; Society for Vascular Nursing; TransAtlantic Inter-Society Consensus; and Vascular Disease Foundation. Circulation *113*, e463–e654.

3. Faglia, E., Clerici, G., Clerissi, J., Gabrielli, L., Losa, S., Mantero, M., Caminiti, M., Curci, V., Lupattelli, T., and Morabito, A. (2006). Early and five-year amputation and survival rate of diabetic patients with critical limb ischemia: data of a cohort study of 564 patients. Eur. J. Vasc. Endovasc. Surg. *32*, 484–490.

4. Faglia, E., Clerici, G., Clerissi, J., Gabrielli, L., Losa, S., Mantero, M., Caminiti, M., Curci, V., Quarantiello, A., Lupattelli, T., and Morabito, A. (2009). Long-term prognosis of diabetic patients with critical limb ischemia: a population-based cohort study. Diabetes Care *32*, 822–827.

5. Carlson, B.M. (1973). The regeneration of skeletal muscle. A review. Am. J. Anat. *137*, 119–149.

6. Bentzinger, C.F., Wang, Y.X., Dumont, N.A., and Rudnicki, M.A. (2013). Cellular dynamics in the muscle satellite cell niche. EMBO Rep. *14*, 1062–1072.

7. Mackie, A.R., and Losordo, D.W. (2011). CD34-positive stem cells: in the treatment of heart and vascular disease in human beings. Tex. Heart Inst. J. *38*, 474–485.

8. Rigato, M., Monami, M., and Fadini, G.P. (2017). Autologous Cell Therapy for Peripheral Arterial Disease: Systematic Review and Meta-Analysis of Randomized, Nonrandomized, and Noncontrolled Studies. Circ. Res. *120*, 1326–1340.

9. Asahara, T., Murohara, T., Sullivan, A., Silver, M., van der Zee, R., Li, T., Witzenbichler, B., Schatteman, G., and Isner, J.M. (1997). Isolation of putative progenitor endothelial cells for angiogenesis. Science *275*, 964–967.

10. Fadini, G.P., and Avogaro, A. (2010). Potential manipulation of endothelial progenitor cells in diabetes and its complications. Diabetes Obes. Metab. *12*, 570–583.

11. Kissel, C.K., Lehmann, R., Assmus, B., Aicher, A., Honold, J., Fischer-Rasokat, U., Heeschen, C., Spyridopoulos, I., Dimmeler, S., and Zeiher, A.M. (2007). Selective functional exhaustion of hematopoietic progenitor cells in the bone marrow of patients with postinfarction heart failure. J. Am. Coll. Cardiol. *49*, 2341–2349.

12. Tepper, O.M., Galiano, R.D., Capla, J.M., Kalka, C., Gagne, P.J., Jacobowitz, G.R., Levine, J.P., and Gurtner, G.C. (2002). Human endothelial progenitor cells from type II diabetics exhibit impaired proliferation, adhesion, and incorporation into vascular structures. Circulation *106*, 2781–2786.

13. Spinetti, G., Fortunato, O., Caporali, A., Shantikumar, S., Marchetti, M., Meloni, M., Descamps, B., Floris, I., Sangalli, E., Vono, R., et al. (2013). MicroRNA-15a and microRNA-16 impair human circulating proangiogenic cell functions and are increased in the proangiogenic cells and serum of patients with critical limb ischemia. Circ. Res. *112*, 335–346.

14. Greco, S., Gaetano, C., and Martelli, F. (2014). HypoxamiR regulation and function in ischemic cardiovascular diseases. Antioxid. Redox Signal. *21*, 1202–1219.

15. Chan, Y.C., Banerjee, J., Choi, S.Y., and Sen, C.K. (2012). miR-210: the master hypoxamir. Microcirculation *19*, 215–223.

16. Ingram, D.A., Mead, L.E., Moore, D.B., Woodard, W., Fenoglio, A., and Yoder, M.C. (2005). Vessel wall-derived endothelial cells rapidly proliferate because they contain a complete hierarchy of endothelial progenitor cells. Blood *105*, 2783–2786.

17. Hirschi, K.K., Ingram, D.A., and Yoder, M.C. (2008). Assessing identity, phenotype, and fate of endothelial progenitor cells. Arterioscler. Thromb. Vasc. Biol. *28*, 1584–1595.

18. Fedchenko, M., Mandalenakis, Z., Rosengren, A., Lappas, G., Eriksson, P., Skoglund, K., and Dellborg, M. (2017). Ischemic heart disease in children and young adults with congenital heart disease in Sweden. Int. J. Cardiol. *248*, 143–148.

19. Zaccagnini, G., Maimone, B., Di Stefano, V., Fasanaro, P., Greco, S., Perfetti, A., Capogrossi, M.C., Gaetano, C., and Martelli, F. (2014). Hypoxia-induced miR-210 modulates tissue response to acute peripheral ischemia. Antioxid. Redox Signal. *21*, 1177–1188.

20. Zaccagnini, G., Maimone, B., Fuschi, P., Maselli, D., Spinetti, G., Gaetano, C., and Martelli, F. (2017). Overexpression of miR-210 and its significance in ischemic tissue damage. Sci. Rep. *7*, 9563.

21. Fasanaro, P., D'Alessandra, Y., Di Stefano, V., Melchionna, R., Romani, S., Pompilio, G., Capogrossi, M.C., and Martelli, F. (2008). MicroRNA-210 modulates endothelial cell response to hypoxia and inhibits the receptor tyrosine kinase ligand Ephrin-A3. J. Biol. Chem. *283*, 15878–15883.

22. Kim, H.W., Haider, H.K., Jiang, S., and Ashraf, M. (2009). Ischemic preconditioning augments survival of stem cells via miR-210 expression by targeting caspase-8-associated protein 2. J. Biol. Chem. *284*, 33161–33168.

23. Arif, M., Pandey, R., Alam, P., Jiang, S., Sadayappan, S., Paul, A., and Ahmed, R.P.H. (2017). MicroRNA-210-mediated proliferation, survival, and angiogenesis promote cardiac repair post myocardial infarction in rodents. J. Mol. Med. (Berl.) *95*, 1369–1385.

24. Hu, S., Huang, M., Li, Z., Jia, F., Ghosh, Z., Lijkwan, M.A., Fasanaro, P., Sun, N., Wang, X., Martelli, F., et al. (2010). MicroRNA-210 as a novel therapy for treatment of ischemic heart disease. Circulation *122* (11, Suppl), S124–S131.

25. Kane, N.M., Meloni, M., Spencer, H.L., Craig, M.A., Strehl, R., Milligan, G., Houslay, M.D., Mountford, J.C., Emanueli, C., and Baker, A.H. (2010). Derivation of endothelial cells from human embryonic stem cells by directed differentiation: analysis of microRNA and angiogenesis in vitro and in vivo. Arterioscler. Thromb. Vasc. Biol. *30*, 1389–1397.

26. Liu, F., Lou, Y.L., Wu, J., Ruan, Q.F., Xie, A., Guo, F., Cui, S.P., Deng, Z.F., and Wang, Y. (2012). Upregulation of microRNA-210 regulates renal angiogenesis mediated by activation of VEGF signaling pathway under ischemia/perfusion injury in vivo and in vitro. Kidney Blood Press. Res. *35*, 182–191.

27. Lou, Y.L., Guo, F., Liu, F., Gao, F.L., Zhang, P.Q., Niu, X., Guo, S.C., Yin, J.H., Wang, Y., and Deng, Z.F. (2012). miR-210 activates notch signaling pathway in angiogenesis induced by cerebral ischemia. Mol. Cell. Biochem. *370*, 45–51.

28. Shoji, T., Nakasa, T., Yamasaki, K., Kodama, A., Miyaki, S., Niimoto, T., Okuhara, A., Kamei, N., Adachi, N., and Ochi, M. (2012). The effect of intra-articular injection of microRNA-210 on ligament healing in a rat model. Am. J. Sports Med. *40*, 2470–2478.

29. Xiao, F., Qiu, H., Zhou, L., Shen, X., Yang, L., and Ding, K. (2013). WSS25 inhibits Dicer, downregulating microRNA-210, which targets Ephrin-A3, to suppress human microvascular endothelial cell (HMEC-1) tube formation. Glycobiology *23*, 524–535.

30. Zeng, L., He, X., Wang, Y., Tang, Y., Zheng, C., Cai, H., Liu, J., Wang, Y., Fu, Y., and Yang, G.Y. (2014). MicroRNA-210 overexpression induces angiogenesis and neurogenesis in the normal adult mouse brain. Gene Ther. *21*, 37–43.

31. Pulkkinen, K., Malm, T., Turunen, M., Koistinaho, J., and Ylä-Herttuala, S. (2008). Hypoxia induces microRNA miR-210 in vitro and in vivo ephrin-A3 and neuronal pentraxin 1 are potentially regulated by miR-210. FEBS Lett. *582*, 2397–2401.

32. Gómez-Maldonado, L., Tiana, M., Roche, O., Prado-Cabrero, A., Jensen, L., Fernandez-Barral, A., Guijarro-Muñoz, I., Favaro, E., Moreno-Bueno, G., Sanz, L., et al. (2015). EFNA3 long noncoding RNAs induced by hypoxia promote metastatic dissemination. Oncogene *34*, 2609–2620.

33. Spinetti, G., Fortunato, O., Cordella, D., Portararo, P., Kränkel, N., Katare, R., Sala-Newby, G.B., Richer, C., Vincent, M.P., Alhenc-Gelas, F., et al. (2011). Tissue kallikrein is essential for invasive capacity of circulating proangiogenic cells. Circ. Res. *108*, 284–293.

34. Cicchillitti, L., Di Stefano, V., Isaia, E., Crimaldi, L., Fasanaro, P., Ambrosino, V., Antonini, A., Capogrossi, M.C., Gaetano, C., Piaggio, G., and Martelli, F. (2012). Hypoxia-inducible factor 1-α induces miR-210 in normoxic differentiating myoblasts. J. Biol. Chem. *287*, 44761–44771.

35. Chang, W., Lee, C.Y., Park, J.H., Park, M.S., Maeng, L.S., Yoon, C.S., Lee, M.Y., Hwang, K.C., and Chung, Y.A. (2013). Survival of hypoxic human mesenchymal stem cells is enhanced by a positive feedback loop involving miR-210 and hypoxia-inducible factor 1. J. Vet. Sci. *14*, 69–76.

36. Kelly, T.J., Souza, A.L., Clish, C.B., and Puigserver, P. (2011). A hypoxia-induced positive feedback loop promotes hypoxia-inducible factor 1alpha stability through miR-210 suppression of glycerol-3-phosphate dehydrogenase 1-like. Mol. Cell. Biol. *31*, 2696–2706.

37. Liu, S.C., Chuang, S.M., Hsu, C.J., Tsai, C.H., Wang, S.W., and Tang, C.H. (2014). CTGF increases vascular endothelial growth factor-dependent angiogenesis in human synovial fibroblasts by increasing miR-210 expression. Cell Death Dis. *5*, e1485.

38. Ceradini, D.J., Kulkarni, A.R., Callaghan, M.J., Tepper, O.M., Bastidas, N., Kleinman, M.E., Capla, J.M., Galiano, R.D., Levine, J.P., and Gurtner, G.C. (2004). Progenitor cell trafficking is regulated by hypoxic gradients through HIF-1 induction of SDF-1. Nat. Med. *10*, 858–864.

39. Jo, D.Y., Rafii, S., Hamada, T., and Moore, M.A. (2000). Chemotaxis of primitive hematopoietic cells in response to stromal cell-derived factor-1. J. Clin. Invest. *105*, 101–111.

40. Ganju, R.K., Brubaker, S.A., Meyer, J., Dutt, P., Yang, Y., Qin, S., Newman, W., and Groopman, J.E. (1998). The alpha-chemokine, stromal cell-derived factor-1alpha, binds to the transmembrane G-protein-coupled CXCR-4 receptor and activates multiple signal transduction pathways. J. Biol. Chem. *273*, 23169–23175.

41. Tu, T.C., Nagano, M., Yamashita, T., Hamada, H., Ohneda, K., Kimura, K., and Ohneda, O. (2016). A Chemokine Receptor, CXCR4, Which Is Regulated by Hypoxia-Inducible Factor 2α, Is Crucial for Functional Endothelial Progenitor Cells Migration to Ischemic Tissue and Wound Repair. Stem Cells Dev. *25*, 266–276.

42. Wang, N., Chen, C., Yang, D., Liao, Q., Luo, H., Wang, X., Zhou, F., Yang, X., Yang, J., Zeng, C., and Wang, W.E. (2017). Mesenchymal stem cells-derived extracellular vesicles, via miR-210, improve infarcted cardiac function by promotion of angiogenesis. Biochim. Biophys. Acta *1863*, 2085–2092.

43. Fasanaro, P., Greco, S., Lorenzi, M., Pescatori, M., Brioschi, M., Kulshreshtha, R., Banfi, C., Stubbs, A., Calin, G.A., Ivan, M., et al. (2009). An integrated approach for experimental target identification of hypoxia-induced miR-210. J. Biol. Chem. *284*, 35134–35143.

44. Filosa, A., Paixão, S., Honsek, S.D., Carmona, M.A., Becker, L., Feddersen, B., Gaitanos, L., Rudhard, Y., Schoepfer, R., Klopstock, T., et al. (2009). Neuron-glia communication via EphA4/ephrin-A3 modulates LTP through glial glutamate transport. Nat. Neurosci. *12*, 1285–1292.

45. Marçola, M., and Rodrigues, C.E. (2015). Endothelial progenitor cells in tumor angiogenesis: another brick in the wall. Stem Cells Int. *2015*, 832649.

46. Haider, H.Kh., and Ashraf, M. (2010). Preconditioning and stem cell survival. J. Cardiovasc. Transl. Res. *3*, 89–102.

47. Kim, J., Kim, M., Jeong, Y., Lee, W.B., Park, H., Kwon, J.Y., Kim, Y.M., Hwang, D., and Kwon, Y.G. (2015). BMP9 Induces Cord Blood-Derived Endothelial Progenitor Cell Differentiation and Ischemic Neovascularization via ALK1. Arterioscler. Thromb. Vasc. Biol. *35*, 2020–2031.

48. Kim, H.W., Jiang, S., Ashraf, M., and Haider, K.H. (2012). Stem cell-based delivery of Hypoxamir-210 to the infarcted heart: implications on stem cell survival and preservation of infarcted heart function. J. Mol. Med. (Berl.) *90*, 997–1010.

49. Devlin, C., Greco, S., Martelli, F., and Ivan, M. (2011). miR-210: More than a silent player in hypoxia. IUBMB Life *63*, 94–100.

50. Deregibus, M.C., Cantaluppi, V., Calogero, R., Lo Iacono, M., Tetta, C., Biancone, L., Bruno, S., Bussolati, B., and Camussi, G. (2007). Endothelial progenitor cell derived microvesicles activate an angiogenic program in endothelial cells by a horizontal transfer of mRNA. Blood *110*, 2440–2448.

51. Kumar, A.H., and Caplice, N.M. (2010). Clinical potential of adult vascular progenitor cells. Arterioscler. Thromb. Vasc. Biol. *30*, 1080–1087.

52. Sahoo, S., Klychko, E., Thorne, T., Misener, S., Schultz, K.M., Millay, M., Ito, A., Liu, T., Kamide, C., Agrawal, H., et al. (2011). Exosomes from human CD34(+) stem cells mediate their proangiogenic paracrine activity. Circ. Res. *109*, 724–728.

53. Jung, K.O., Youn, H., Lee, C.H., Kang, K.W., and Chung, J.K. (2017). Visualization of exosome-mediated miR-210 transfer from hypoxic tumor cells. Oncotarget *8*, 9899–9910.

54. King, H.W., Michael, M.Z., and Gleadle, J.M. (2012). Hypoxic enhancement of exosome release by breast cancer cells. BMC Cancer *12*, 421.

55. Tadokoro, H., Umezu, T., Ohyashiki, K., Hirano, T., and Ohyashiki, J.H. (2013). Exosomes derived from hypoxic leukemia cells enhance tube formation in endothelial cells. J. Biol. Chem. *288*, 34343–34351.

56. Wang, Y., Zhang, L., Li, Y., Chen, L., Wang, X., Guo, W., Zhang, X., Qin, G., He, S.H., Zimmerman, A., et al. (2015). Exosomes/microvesicles from induced pluripotent

stem cells deliver cardioprotective miRNAs and prevent cardiomyocyte apoptosis in the ischemic myocardium. Int. J. Cardiol. *192*, 61–69.

57. Barile, L., Lionetti, V., Cervio, E., Matteucci, M., Gherghiceanu, M., Popescu, L.M., Torre, T., Siclari, F., Moccetti, T., and Vassalli, G. (2014). Extracellular vesicles from human cardiac progenitor cells inhibit cardiomyocyte apoptosis and improve cardiac function after myocardial infarction. Cardiovasc. Res. *103*, 530–541.

58. Namazi, H., Mohit, E., Namazi, I., Rajabi, S., Samadian, A., Hajizadeh-Saffar, E., Aghdami, N., and Baharvand, H. (2018). Exosomes secreted by hypoxic cardiosphere-derived cells enhance tube formation and increase pro-angiogenic miRNA. J. Cell. Biochem. *119*, 4150–4160.

59. Zhu, J., Lu, K., Zhang, N., Zhao, Y., Ma, Q., Shen, J., Lin, Y., Xiang, P., Tang, Y., Hu, X., et al. (2017). Myocardial reparative functions of exosomes from mesenchymal stem cells are enhanced by hypoxia treatment of the cells via transferring microRNA-210 in an nSMase2-dependent way. Artif. Cells Nanomed. Biotechnol. , Published online November 16, 2017. https://doi.org/10.1080/21691401.2017.1388249.

60. Au, P., Daheron, L.M., Duda, D.G., Cohen, K.S., Tyrrell, J.A., Lanning, R.M., Fukumura, D., Scadden, D.T., and Jain, R.K. (2008). Differential in vivo potential of endothelial progenitor cells from human umbilical cord blood and adult peripheral blood to form functional long-lasting vessels. Blood *111*, 1302–1305.

61. Shin, J.Y., Yoon, J.K., Noh, M.K., Bhang, S.H., and Kim, B.S. (2016). Enhancing Therapeutic Efficacy and Reducing Cell Dosage in Stem Cell Transplantation Therapy for Ischemic Limb Diseases by Modifying the Cell Injection Site. Tissue Eng. Part A *22*, 349–362.

62. Elshaer, S.L., Lorys, R.E., and El-Remessy, A.B. (2016). Cell Therapy and Critical Limb Ischemia: Evidence and Window of Opportunity in Obesity. Obes. Control Ther. *3*, 121.

63. Foubert, P., Silvestre, J.S., Souttou, B., Barateau, V., Martin, C., Ebrahimian, T.G., Leré-Déan, C., Contreres, J.O., Sulpice, E., Levy, B.I., et al. (2007). PSGL-1-mediated activation of EphB4 increases the proangiogenic potential of endothelial progenitor cells. J. Clin. Invest. *117*, 1527–1537.

64. Lee, S.H., Lee, K.B., Lee, J.H., Kang, S., Kim, H.G., Asahara, T., and Kwon, S.M. (2015). Selective Interference Targeting of Lnk in Umbilical Cord-Derived Late Endothelial Progenitor Cells Improves Vascular Repair, Following Hind Limb Ischemic Injury, via Regulation of JAK2/STAT3 Signaling. Stem Cells *33*, 1490–1500.

65. Pfaffl, M.W. (2001). A new mathematical model for relative quantification in real-time RT-PCR. Nucleic Acids Res. *29*, e45.

66. Caporali, A., Meloni, M., Völlenkle, C., Bonci, D., Sala-Newby, G.B., Addis, R., Spinetti, G., Losa, S., Masson, R., Baker, A.H., et al. (2011). Deregulation of microRNA-503 contributes to diabetes mellitus-induced impairment of endothelial function and reparative angiogenesis after limb ischemia. Circulation *123*, 282–291.

67. Thery, C., Amigorena, S., Raposo, G., and Clayton, A. (2006). Isolation and characterization of exosomes from cell culture supernatants and biological fluids. Curr. Protoc. Cell Biol. *30*, 3.22.1–3.22.29.

68. Dragovic, R.A., Gardiner, C., Brooks, A.S., Tannetta, D.S., Ferguson, D.J., Hole, P., Carr, B., Redman, C.W., Harris, A.L., Dobson, P.J., et al. (2011). Sizing and phenotyping of cellular vesicles using Nanoparticle Tracking Analysis. Nanomedicine (Lond.) *7*, 780–788.

69. Emanueli, C., Minasi, A., Zacheo, A., Chao, J., Chao, L., Salis, M.B., Straino, S., Tozzi, M.G., Smith, R., Gaspa, L., et al. (2001). Local delivery of human tissue kallikrein gene accelerates spontaneous angiogenesis in mouse model of hindlimb ischemia. Circulation *103*, 125–132.

70. Perfetti, A., Greco, S., Cardani, R., Fossati, B., Cuomo, G., Valaperta, R., Ambrogi, F., Cortese, A., Botta, A., Mignarri, A., et al. (2016). Validation of plasma microRNAs as biomarkers for myotonic dystrophy type 1. Sci. Rep. *6*, 38174.

YMTHE, Volume *26*

Supplemental Information

miR-210 Enhances the Therapeutic Potential of Bone-Marrow-Derived Circulating Proangiogenic Cells in the Setting of Limb Ischemia

Marie Besnier, Stefano Gasparino, Rosa Vono, Elena Sangalli, Amanda Facoetti, Valentina Bollati, Laura Cantone, Germana Zaccagnini, Biagina Maimone, Paola Fuschi, Daniel Da Silva, Michele Schiavulli, Sezin Aday, Massimo Caputo, Paolo Madeddu, Costanza Emanueli, Fabio Martelli, and Gaia Spinetti

Supplemental Figures

Besnier, Gasparino, Vono et al. Title: MicroRNA-210 enhances the therapeutic potential of bone marrow-derived circulating proangiogenic cells in the setting of limb ischemia.

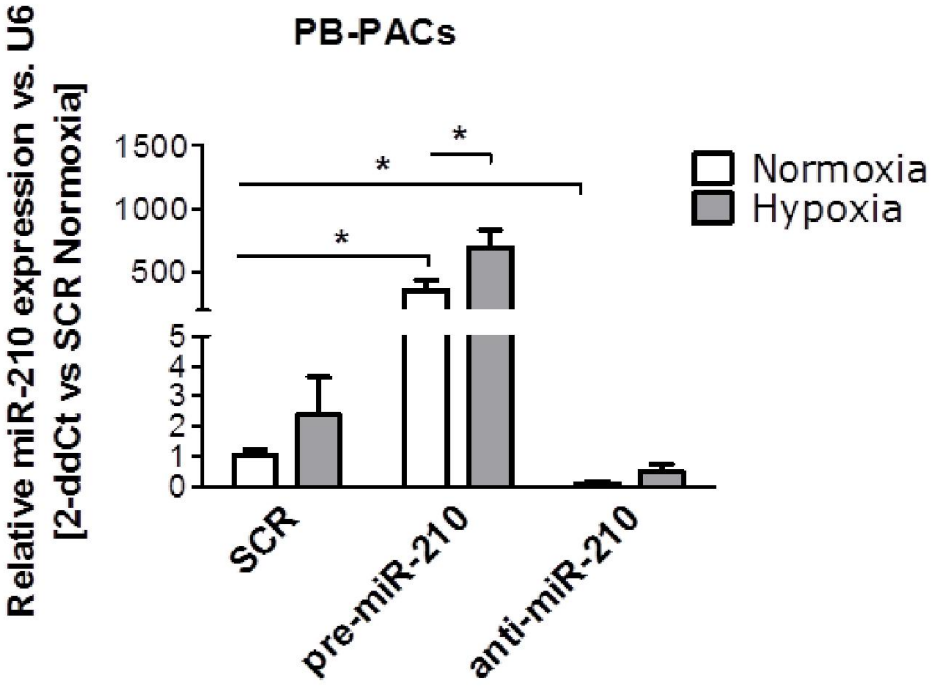

Supplementary figure I. Efficiency of miR-210 modulation in human PB-PACs. PB-PACs were transfected with pre-miR-210, anti-mir-210 or a scramble control sequence. Bar graph of relative miR-210 expression in control (scramble, SCR), pre-miR-210 and anti-miR-210 transfected PB-PACs. *p<0.05. Data shown as mean±SEM, N=4 donors. U6 snRNA used as a normalyzer

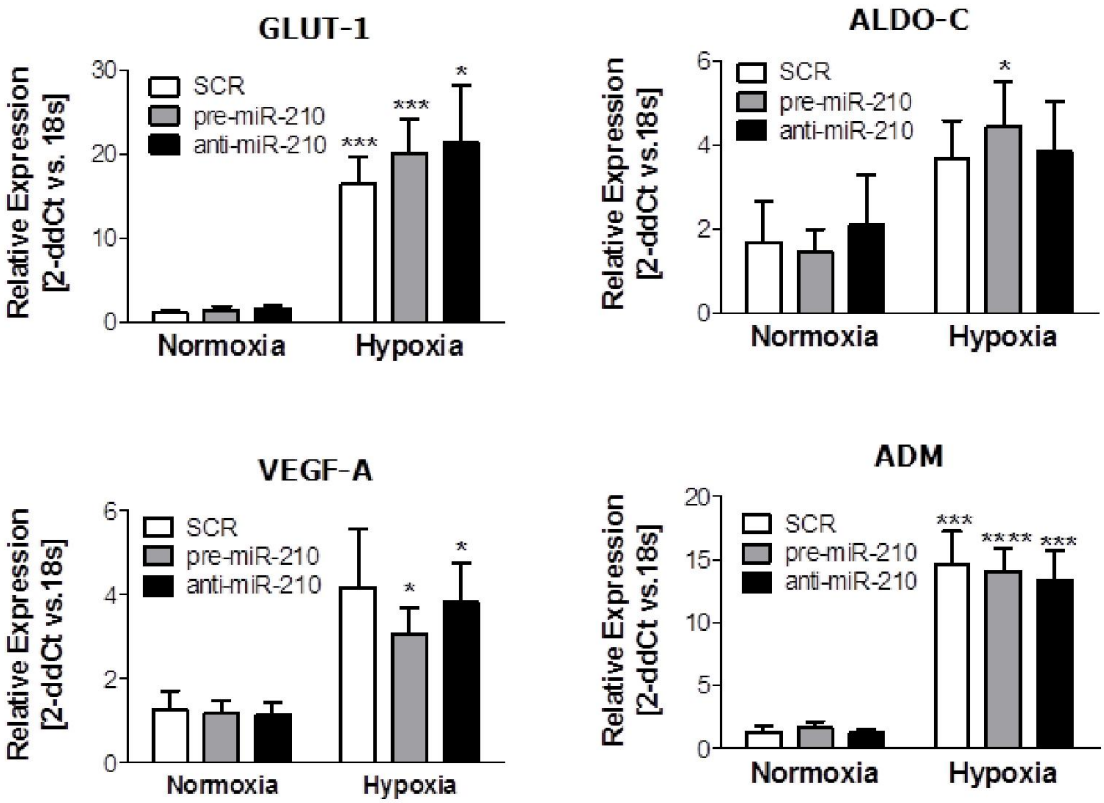

Supplementary figure II. miR-210 modulation is not associated with changes in the HIF-1a targets in adult PACs. Cells were transfected with pre-miR-210, anti-mir-210 or a scramble. After 48h, mRNA expression of *GLUT-1, ALDO-C, VEGF-A* and *ADM* was assessed by qRT-PCR over 18s housekeeping gene. Bar graph of average relative abundance of HIF1a-associated genes measured by real time q-PCR. *p<0.05; ***p<0.001; ****p<0.0001 vs. Normoxia. Data shown as mean±SEM, N=6 donors.

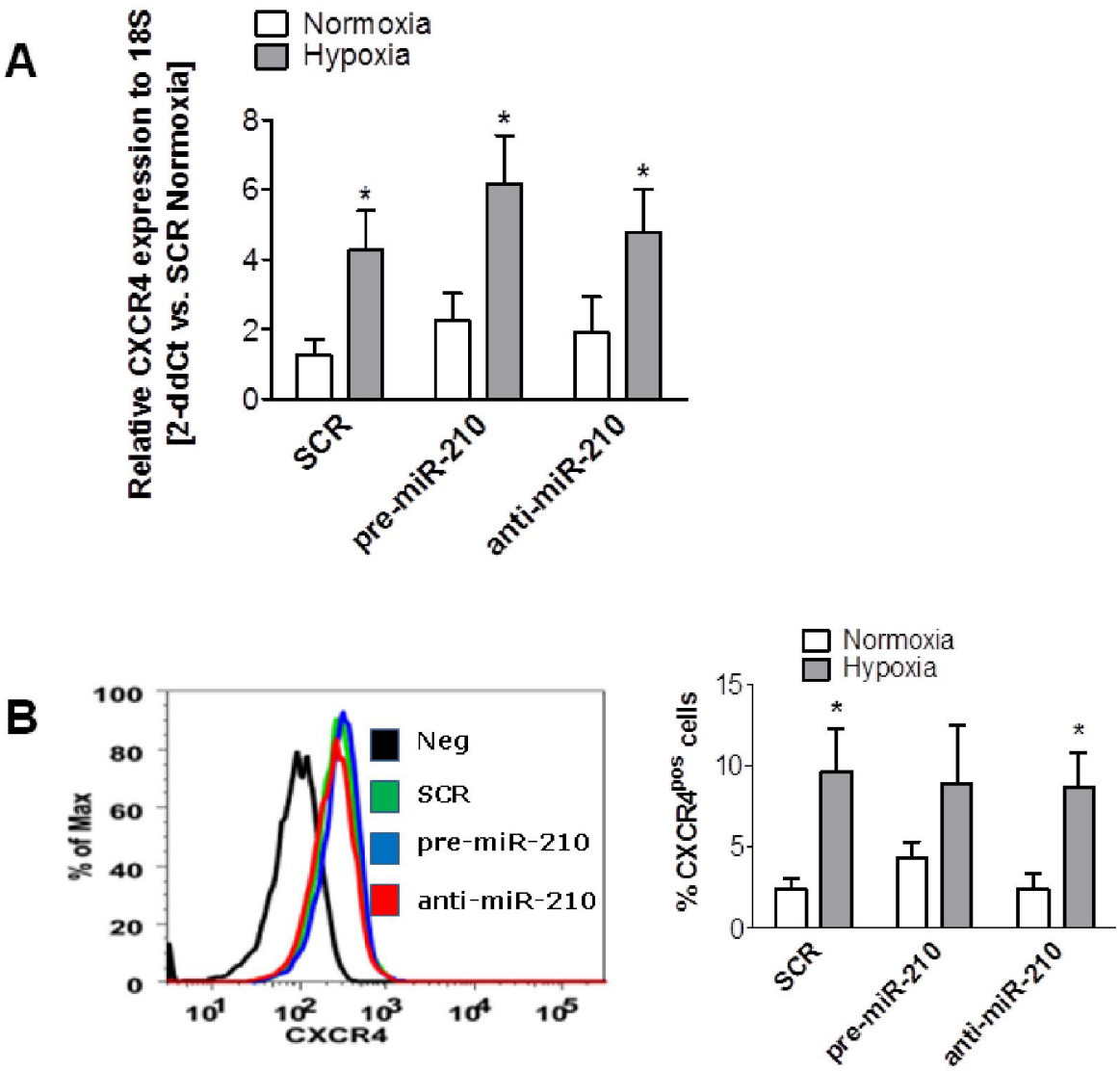

Supplementary figure III. The expression of the SDF-1a receptor CXCR4 is not altered by miR-210 expressional changes in PB-PACs cultured under hypoxia or normoxia. A) Bar graph showing CXCR4 mRNA expression in PACs engineered with pre- or anti-miR-210 and scramble (SCR). **B**) Representative flow cytometric analysis (left) and graph of average percentage of CXCR4-positive PB-PACs (right). Data shown as mean±SEM, N=6 donors. *p<0.05 vs. normoxia in both panels.

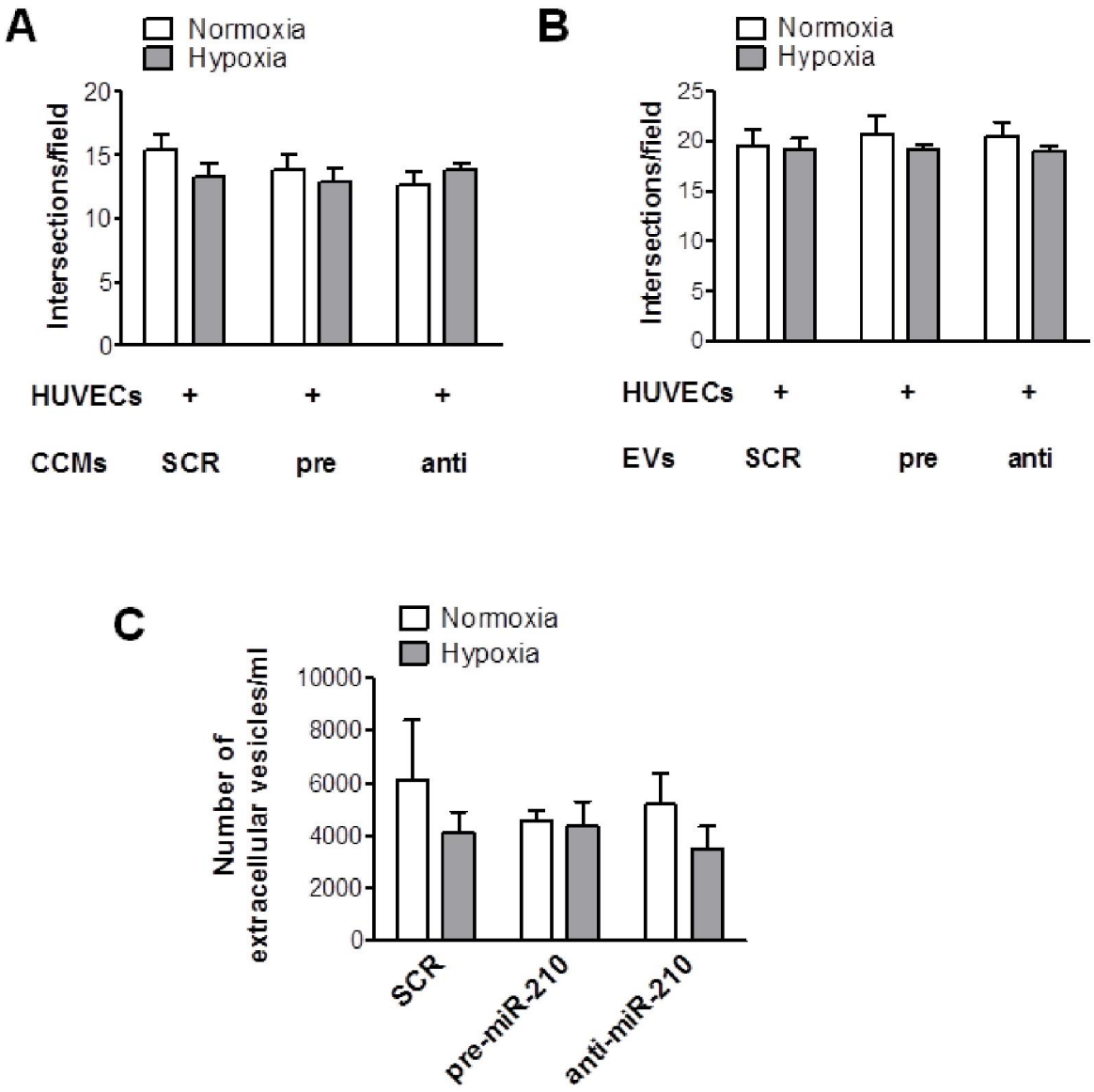

Supplementary figure IV. **Characterization of the PB-PACs paracrine activity in the Matrigel assay.** Bar graph shows the number of HUVEC intersections on Matrigel, when exposed to the **A**) unfractioned conditioned cell medium (CCM) or **B**) the CCM-derived extracellular vesicles (EVs) of engineered PACs kept under normoxia or hypoxia. **C**) The abundance of secreted EVs does not change with miR-210 expressional changes. Bar graph of average EV abundance measured by NanoSight in PAC CCMs . Data shown as mean±SEM, N=4 donors for all experiments.

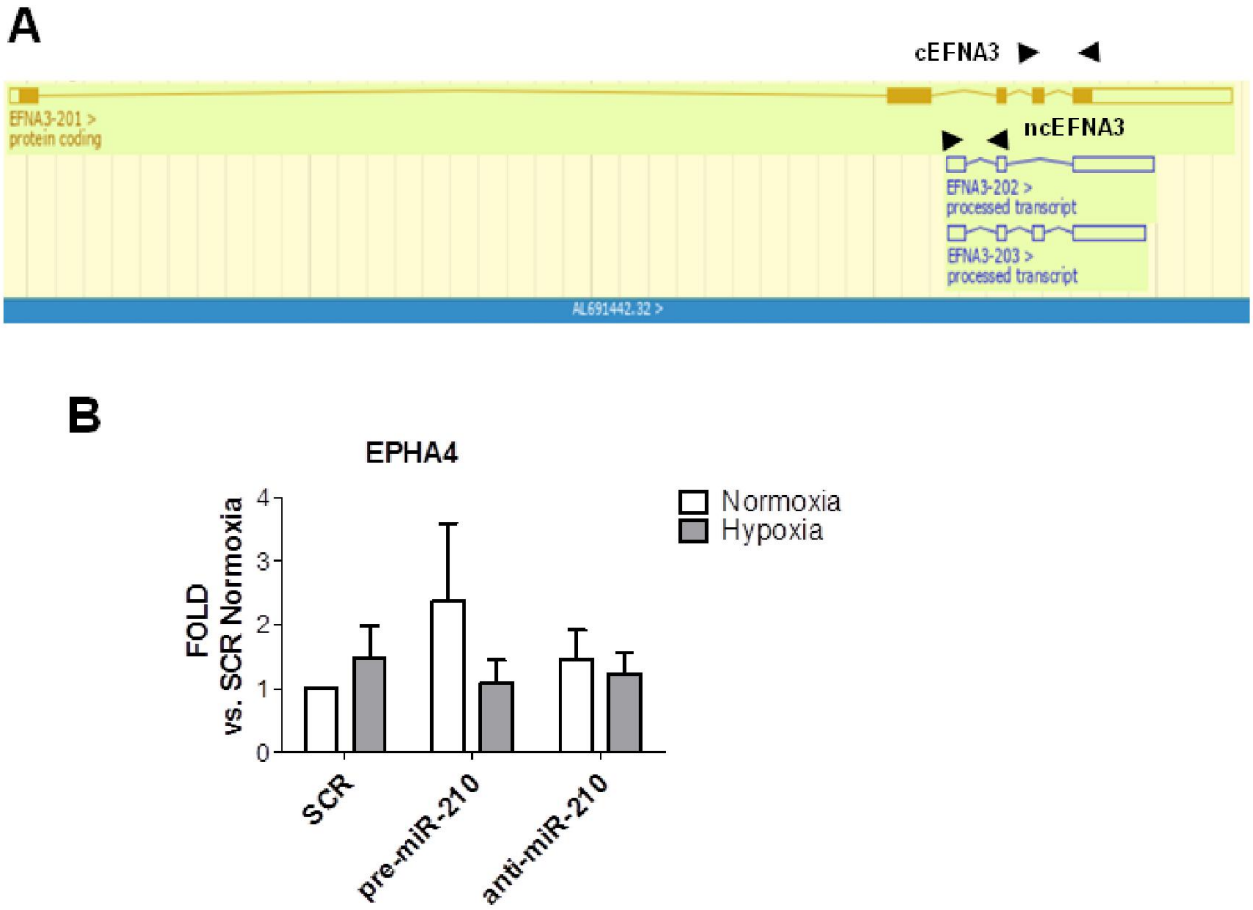

Supplementary figure V. Analysis of hypoxia and miR-210 modulation on coding and non-coding EFNA3 isoforma. Coding (cEFNA3) and non-coding (ncEFNA3) EFNA3 isoforms were analyzed by qPCR in PB-PACs. **A**) The figure shows the position of cEFNA3 and ncEFNA3A primers on the EFNA3 gene (Ensembl sequence). **B**) Analysis of EFNA3 receptor EPHA4 expression in PB-PACs under normoxia and hypoxia following miR-210 modulation. Data expressed as mean±SEM of qPCR analysis vs. UCB as housekeeping gene, N=4 donors.

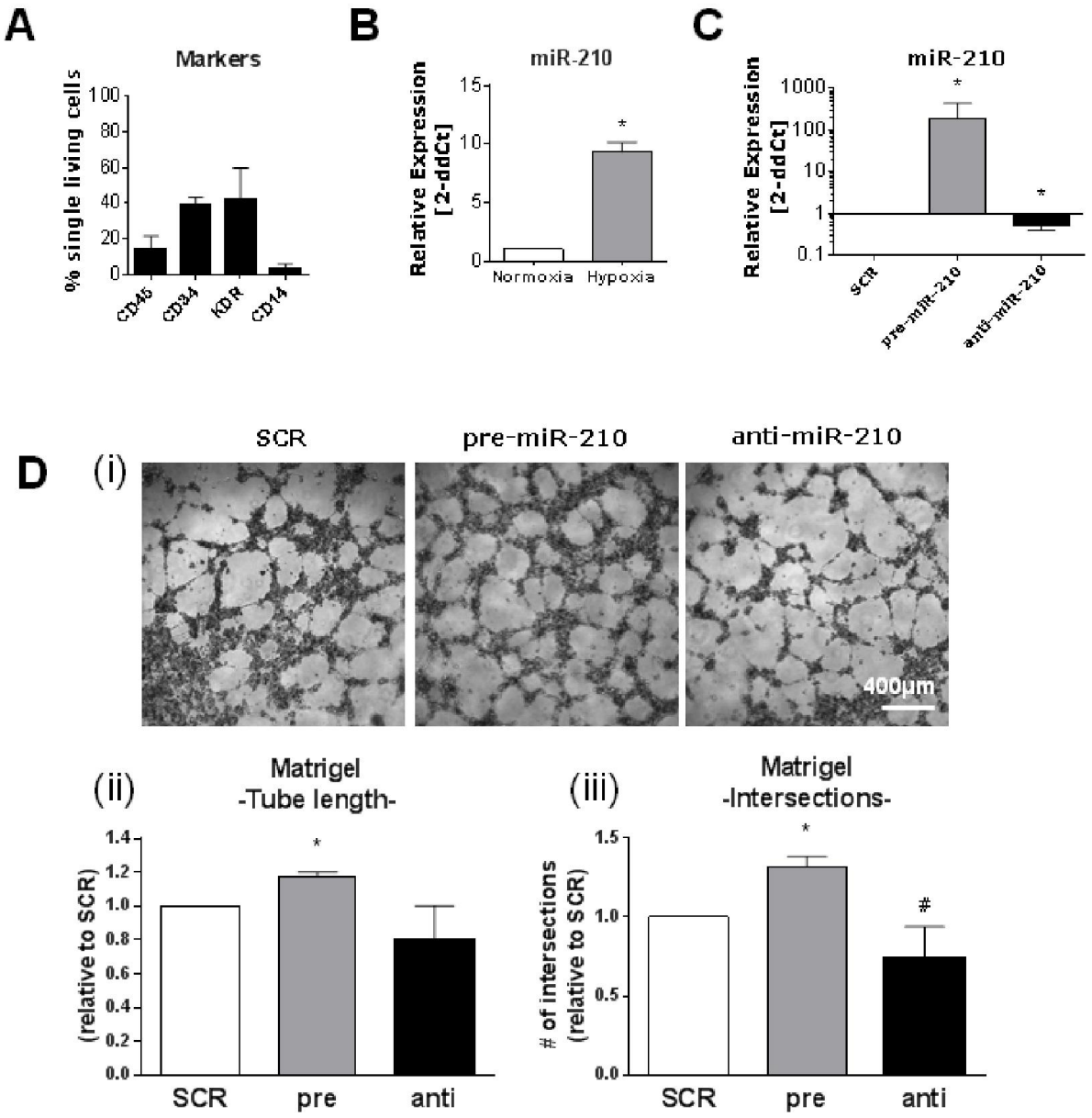

Supplementary figure VI. Characterisation of umbilical cord (UBC)-PACs and effect of modulation of miR-210 expression on PACs activity. A) Flow cytometric measurement of progenitor markers, expressed in %, of single and living cells (data shown as mean±SEM, N=3). **B**) Relative expresson of miR-210 under normoxia and hypoxia or **C**) after transfection with scramble (SCR), pre-miR-210 (pre) and anti-miR-210 (anti) in UBC-PACs. Bar graph of relative expression to snU6 shown as mean±SEM, (N=3). **D**) miR-210 facilitates HUVECs networking: (**i**) Representative pictures, scale bar: 400µm. Bar graph of average endothelial tube length (**ii**) and intersection (**iii**) ±SEM of HUVECs cultured in the presence of UBC-PAC. Data are represented as relative to each SCR control donor (N=3). *p<0.05 *vs.* SCR control or normoxia control. $^{\#}$p<0.05 *vs.* pre-miR-210 condition.

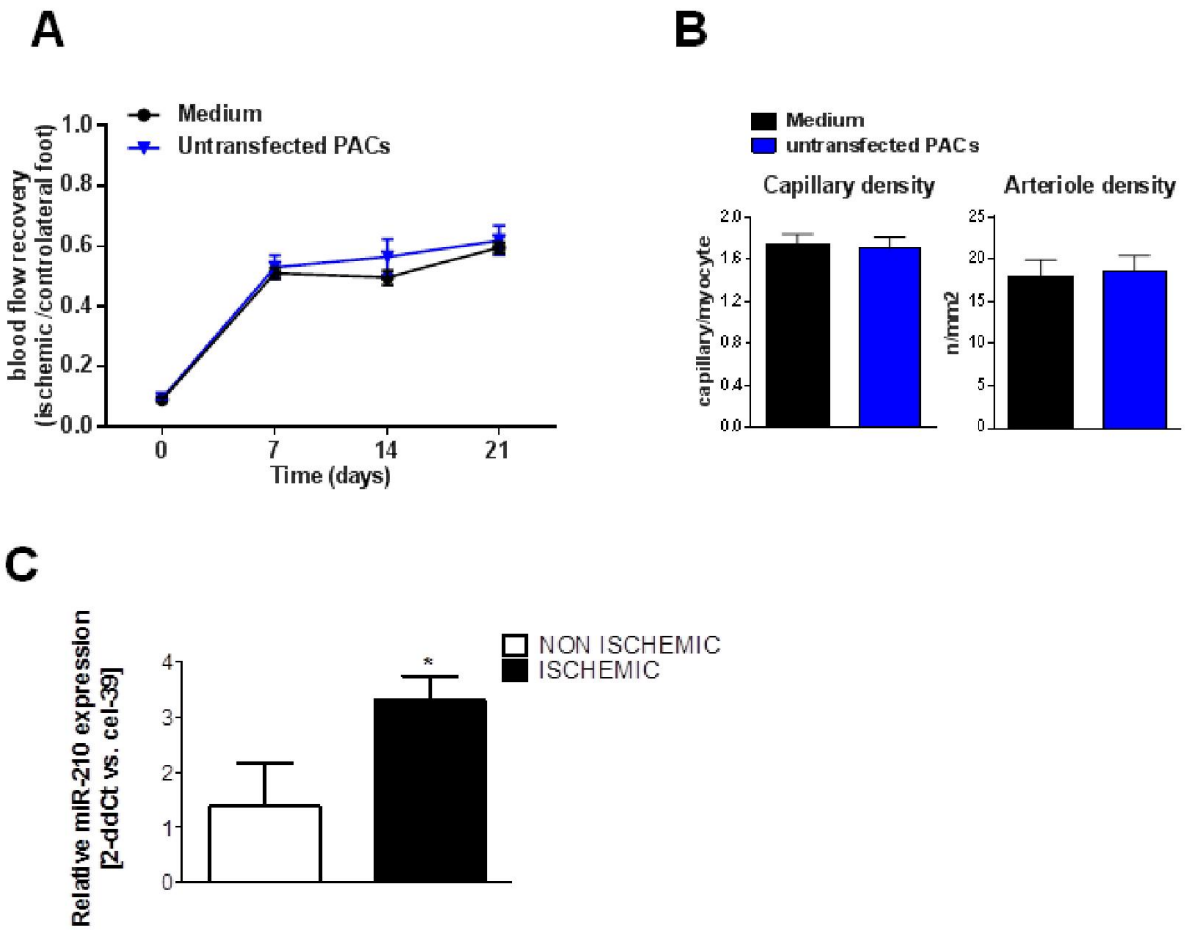

Supplementary figure VII. Untransfected PACs therapy does not increase vascular repair in our immunocompromised mouse model of unilateral limb ischemia. Untransfected PACs or fresh cell medium were injected in the ischemic adductor muscle of mice with surgically induced unilateral limb ischemia. **A**) Posti-schemic blood flow recovery: Time course of blood flow recovery (calculated as the ratio of blood flow in ischemic to contralateral foot) measured by color laser Doppler (n=11-12/group). **B**) Analyses of capillary and arteriole density in ischemic muscles at 21 days post-ischemia (n=6/group). **C**) Bar graph of average relative expression of mature miR-210 normalized by cel-miR-39 spike-in, in the plasma of CD57Bl6 mice non ischemic (N=3) and 3 days after hindlimb ischemia (ischemic, N=5). * $p<0.05$. Data are expressed as mean±SEM.